AD-A048 271 AIR FORCE GEOPHYSICS LAB HANSCOM AFB MASS F/G 20/14
THE DISTRIBUTION OF THUNDERSTORM DAYS, LIGHTNING DISCHARGES, AN--ETC(U)
MAY 77 W B FREEMAN
UNCLASSIFIED AFGL-TR-77-0112 NL

1 OF 1
AD
AD48271

END
DATE FILMED
1-78
DDC

AFGL-TR-77-0112
SPECIAL REPORTS, NO. 203

The Distribution of Thunderstorm Days, Lightning Discharges, and the Incidence of Lightning Discharge Derived From VLF Sferics Data

WILLIAM B. FREEMAN, Jr., Major, USAF

17 May 1977

AIR FORCE GEOPHYSICS LABORATORY
HANSCOM AFB, MASSACHUSETTS 01731

AIR FORCE SYSTEMS COMMAND, USAF

This report has been reviewed by the ESD Information Office (OI) and is releasable to the National Technical Information Service (NTIS).

This technical report has been reviewed and is approved for publication.

FOR THE COMMANDER

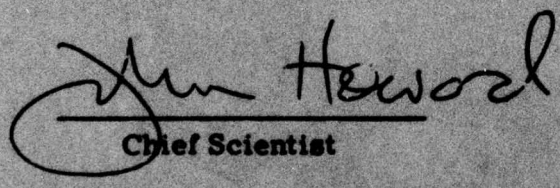

Chief Scientist

Qualified requestors may obtain additional copies from the Defense Documentation Center. All others should apply to the National Technical Information Service.

Unclassified

SECURITY CLASSIFICATION OF THIS PAGE (When Data Entered)

REPORT DOCUMENTATION PAGE

READ INSTRUCTIONS BEFORE COMPLETING FORM

1. REPORT NUMBER: AFGL-TR-77-0112, AFGL-SR-203	2. GOVT ACCESSION NO. / 3. RECIPIENT'S CATALOG NUMBER
4. TITLE (and Subtitle): THE DISTRIBUTION OF THUNDERSTORM DAYS, LIGHTNING DISCHARGES, AND THE INCIDENCE OF LIGHTNING DISCHARGE DERIVED FROM VLF SFERICS DATA	5. TYPE OF REPORT & PERIOD COVERED: N/A
	6. PERFORMING ORG. REPORT NUMBER: SR No. 203 ✓
7. AUTHOR(s): William B. Freeman, Jr. ~~Major, USAF~~*	8. CONTRACT OR GRANT NUMBER(s): N/A
9. PERFORMING ORGANIZATION NAME AND ADDRESS: AFGL Staff Meteorology Office (WE) ✓ Hanscom AFB Massachusetts 01731	10. PROGRAM ELEMENT, PROJECT, TASK AREA & WORK UNIT NUMBERS: N/A
11. CONTROLLING OFFICE NAME AND ADDRESS: AFGL Staff Meteorology Office (WE) Hanscom AFB Massachusetts 01731	12. REPORT DATE: 17 May 1977 / NUMBER OF PAGES: 89 pp.
14. MONITORING AGENCY NAME & ADDRESS (if different from Controlling Office)	15. SECURITY CLASS. (of this report): Unclassified / 15a. DECLASSIFICATION/DOWNGRADING SCHEDULE

16. DISTRIBUTION STATEMENT (of this Report)

Approved for public release; distribution unlimited.

17. DISTRIBUTION STATEMENT (of the abstract entered in Block 20, if different from Report)

DDC RECEIVED JAN 12 1978 F

18. SUPPLEMENTARY NOTES

*AFGL and ESD Staff Meteorology Office

19. KEY WORDS (Continue on reverse side if necessary and identify by block number)

Lightning
Sferics
Thunderstorm
Lightning discharge
Thunderstorm days

20. ABSTRACT (Continue on reverse side if necessary and identify by block number)

Distributions were developed for 1972 in the Eastern Hemisphere of thunderstorm days (January, April, July, and October), the incidence of lightning discharge (January and April), and the areal concentration of lightning discharge (yearly). These analyses were based on a review of *sferics* data. Charts of thunderstorm days differed significantly from mean charts of the World Meteorological Organization (WMO), especially over the oceans, North Africa, Arabia, the Mediterranean Sea, and Southeast China.

DD FORM 1 JAN 73 1473 EDITION OF 1 NOV 65 IS OBSOLETE

Unclassified

SECURITY CLASSIFICATION OF THIS PAGE (When Data Entered)

409578

20. Abstract (Continued)

These areas of sparse data in the WMO compilation have been covered in this investigation. The tentative, first estimate of the distribution of lightning discharges over a large area of Earth differed significantly from the distribution of thunderstorm days for April and July, but the two distributions were similar for January and October. Centers of relatively high occurrence of lightning discharge on a yearly basis were located over South Africa, the Mediterranean Sea, Arabia, Southeast China, Southeast Asia, and Australia. The occurrence of lightning discharge was shown to follow Sun northward from January to the maximum poleward thrust in July. The occurrence of lightning discharge receded equatorward from July to the end of fall in December. The most reliable planetary-scale estimate of the average incidence of lightning discharge was 4.2×10^{-5} km^{-2} sec^{-1} for the Northern Hemisphere (0-179E) in January 1972 and 3.0×10^{-5} km^{-2} sec^{-1} for April 1972. There was evidence that, in general, the areal concentration of lightning discharge in the Northern Hemisphere (0-179E) decreased with geographic latitude.

0.000042 per km per sec

0.000030 per km per sec

Preface

This research effort was approved by the Meteorology Department of Texas A&M University in May 1974, in partial fulfillment of the requirements for the Master of Science degree. The work was sponsored and financed by the United States Air Force. The author acknowledges the professional guidance given by Professor George L. Huebner, Committee Chairman, and also by Professors John F. Griffiths and Dušan Djurić of Texas A&M University. Dr. Donald R. Fitzgerald of the Air Force Geophysics Laboratory reviewed the thesis and recommended that Appendix A be included in this report as an addition.

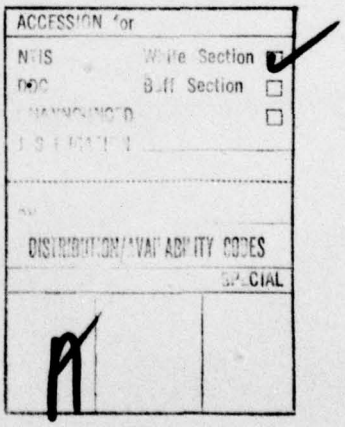

Contents

Illustrations

Illustrations

Tables

Tables

The Distribution of Thunderstorm Days, Lightning Discharges, and the Incidence of Lightning Discharge Derived From VLF Sferics Data

1. INTRODUCTION

1.1 Need for This Investigation

Scientists have studied electrical activity in the atmosphere for more than 200 years,[1] yet there remain gaps in our knowledge of the nature of these complex phenomena. The lightning discharge is perhaps the most dramatic electrical event in nature and one of the most misunderstood.[2] There is a need to understand better all aspects of the lightning discharge, including its climatology.

Horner[3] stated that there is a requirement in radio science for a better understanding of the temporal and spatial distribution of the areal density of lightning discharge. He wrote:

> If a more complete knowledge existed of the densities of lightning discharges in different parts of the world, it could be coupled with a knowledge of the energy radiated by an average discharge to give the world distribution of radiated power. Hitherto this distribution has

(Received for publication 17 May 1977)

1. Chi-Chen, L., and Chi-Zhang, L. (1966) AFCRL, Contract AF19(628)-5073, Emm-67-165 Translations, Translated from Acta Meteorologica Sinica 36:275-279.
2. Viemeister, P. E. (1961) The Lightning Book, Doubleday, New York, 316 pp.
3. Horner, F. (1964) Advances in Radio Research, Vol. 2, Academic Press, New York, pp. 121-204.

been assumed to follow the distribution of thunderstorm days, for want of a better index.

Martin and Hildebrand[4] have expressed the need for a climatology of thunderstorm and lightning parameters, as stated:

> Many scientific and engineering disciplines have an interest in the geographic distribution of thunderstorm activity . . . In much of this work there is need for information regarding the expected thunderstorm activity at various geographic locations around the world to enable assessment of its contribution to the total atmospheric noise level at any other geographic location. On a worldwide basis, knowledge concerning the number and location of lightning discharges, which create large amounts of radio frequency energy, is still very meager and based to a large extent upon studies made in 1925.

Byers[5] explained that meteorologists have a special interest in atmospheric, electrical phenomena:

> The main feature that distinguishes meteorology from the other sciences that might concern themselves with the atmosphere is its emphasis on circulations. These circulations, ranging from small turbulent eddies to the air flow over the planet as a whole, influence the distribution of electrical properties. Thus, a two-way relation between lightning, as well as all other electrical phenomena, and meteorological conditions exists.

A better knowledge of the distribution of lightning discharges would be useful in the planning of aircraft routes, especially over remote areas.

Extensive data are available on some aspects of the spatial and temporal occurrence of thunderstorms. There is a relative paucity of information on the occurrence of lightning.

1.2 Literature Review: Statistics of Thunderstorm and Lightning Parameters

A thunderstorm day is defined as a local day on which thunder is heard at a weather station. The observation of lightning without the sonic noise that it produces (thunder) is not a sufficient criterion for a thunderstorm day to be recorded.[6] The thunderstorm day is the only planetary-scale estimate of thunderstorm occurrence that is available. Although a useful statistic, it has obvious deficiencies.

4. Martin, J.N., and Hildebrand, V.W. (1965) NOLC Rept. 628 Project No. WR5-0062, Naval Ordnance Laboratory, Corona, Calif., 95 pp.
5. Byers, H.R. (1965) Problems of Atmospheric and Space Electricity, Elsevier Pub. Co., Amsterdam, pp. 491-496.
6. World Meteorological Organization (1953) Part 1, Publ. No. 21, TP 6.

Thunderstorm-day data provide no estimate of diurnal variation, duration, or electrical intensity of thunderstorms. A thunderstorm day is recorded at a station whether there occurred a single, isolated thunderstorm or several thunderstorms during the day. Moreover, the efficacy of thunderstorm-day statistics is based on the obviously false premise that thunder always is heard no matter where it occurs.

Personnel of the World Meteorological Organization (WMO) compiled the thunderstorm-day statistics from raw material submitted by the meteorological services of the member nations. The following quotation is taken from Part 2 of the data presentation.[7]

> It should be made clear that this project is not a detailed climatological study of thunderstorm activity over the world ... The maps cannot be considered to be in any way final; they are subject to revision in light of new data.

Brooks,[8] in a classic paper, pointed out that thunderstorm-day records may be inaccurate. He said:

> Thunderstorms which pass directly over the station may be noted, but those which occur at a distance of several miles are often ignored; this is especially the case in tropical stations where thunderstorms are severe but extremely local – at certain times of the day in the rainy season distant thunder is so common that it simply does not occur to the observer to enter it in the register – in fact, he may not be consciously aware of its occurrence . . .

In the same paper, Brooks[8] estimated from a review of station reports that there are approximately 1800 thunderstorms in existence on Earth at any one time and that roughly 100 discharges occur per second. Heydt and Volland[9] used a heterodyne type of receiver to study the amplitude spectra of received atmospherics. They estimated, based on counts of signals at frequencies of 5 kHz, 10 kHz, and 40 kHz that approximately 120 discharges occur per second. This result is in close agreement with that of Brooks, especially when one considers the disparate methods of analysis.

Aiya[10] used lightning flash counters to estimate that a local thunderstorm in India lasts 3 hours on the average and produces about one discharge per km^2. This corresponds to an incidence of discharge of approximately 9×10^{-5} km^{-2} sec^{-1}.

---

7. World Meteorological Organization (1956) Part 2, Publ. No. 21, TP 6.
8. Brooks, C.E.P. (1925) Met. Office Geophys. Mem. and Profl. Notes, No. 24, London, 147-164.
9. Heydt, G., and Volland, H. (1964) J. Atmos. Terr. Phys. 26:85-104.
10. Aiya, S.V.C. (1968) Electro-Technology, J. Soc. Electronic Engineers (Bangalore) 12:(No. 1):1-12.

Horner[11] reviewed data based on various sources (for example, lightning flash counters, strikes to power lines, and radio noise) and estimated that the incidence for the "main thunderstorm areas" of the world is 10^{-5} km^{-2} sec^{-1}. He also estimated that the incidence for the world as a whole is of the order 10^{-6} km^{-2} sec^{-1}. Neither Aiya nor Horner indicated over what period the respective estimates of incidence were averaged. By assuming that on the average one thunderstorm occurs per thunderstorm day, one may infer from Brook's work[8] that the incidence of discharge is of the order of 10^{-4} km^{-2} sec^{-1} for the world as a whole.

1.2.1 THE LIGHTNING DISCHARGE

Lightning, in general, is the visible electrical discharge produced by thunderstorms. The lightning discharge is a series of electrical processes by which charge is transferred between centers of opposite polarity.[12] Lightning discharges almost always are accompanied by thunder. In April 1855, five "brilliant flashes" of lightning were seen to strike the Washington Monument without any observation of thunder. However, observations of this nature are extremely rare.[2] The types of discharge which are within the scope of this study include cloud-to-ground and cloud discharges. Other types of discharge (for example, cloud-to-air, and cloud-to-cloud) occur very rarely.[13, 2]

The cloud-to-ground discharge is a composite and complicated event. It may be studied conveniently in three stages: (1) The initial stage of the step leaders forms the conductive path to ground and ends at the first return stroke; (2) the intermediate stage includes all return strokes; and (3) the final stage comprises the residual variations in electric field after the last return stroke.[14]

The leaders follow a stepped, tortuous trajectory from the cloud to the ground and ionize a conductive path which typically connects the negative center of charge in the cloud to an induced, positive center on the ground. The return stroke gives off light as it apparently moves upward from ground to cloud. This visual display is popularly termed "lightning." The return stroke actually moves downward, typically carrying negative charges from cloud to ground.[15]

---

11. Horner, F. (1965) Planet Space Sci. 13:1137-1150.
12. Huschke, R.E., Ed. (1959) Glossary of Meteorology, Am. Meteor. Soc., Boston, 638 pp.
13. Ishikawa, H. (1960) Proc. Res. Inst. Atmos., Nagoya Univ., 8A:1-274.
14. Pierce, E.T. et al (1962) Final Rept. SRI Project No. 3738, Contract No. AF33(657)-7009, Stanford Research Institute, Menlo Park, Calif., 132 pp.
15. Chalmers, J.A. (1967) Atmospheric Electricity, 2nd ed., Pergamon, New York, 515 pp.

There are multiple return strokes in most cloud-to-ground discharges. The number of return strokes may vary from one to as many as 20.[16, 17, 18, 19] Pierce[20] developed empirical rules for the variation with latitude of the average number of return strokes per cloud-to-ground discharge and the proportion of all discharges that go to ground. He found that with geographic latitude the proportion of discharges-to-ground increases, and the number of return strokes per discharge decreases.

The nature of the cloud discharge is not clearly understood. Smith[21] observed that most (56 percent) cloud discharges transfer negative charge upward from a negative center of charge near the cloud base to a positive center above. Ogawa and Brook[22] observed that the direction of propagation of charge was predominantly (75 percent of cases studied) from the positive center of charge downward to the negative center of charge. Takagi[23] observed in Japan that the main process of cloud discharge involves a positive streamer that propagates downward from a positive to a negative center of charge. Moyer[24] observed from aloft a line storm in which about 75 percent of the discharges appeared to parallel the bases of single clouds with the stroke typically emerging from one extremity and re-entering an opposite extremity. This observation was made on 12 November 1972 at a location south of Dallas, Texas.

1.2.2 ATMOSPHERICS

Atmospherics are electromagnetic signals which emanate from lightning discharges.[15] The term "atmospherics" is frequently shortened to "sferics." Popov,[25] working at the Pavlovsk Magnetic and Meteorological Observatory, was the first investigator to study the phenomena with the use of a detector. Recent advances in sferics work have been largely refinements and extensions of pioneer work accomplished before 1940. According to Horner,[3] the principal early workers were Appleton and Watson-Watt in the United Kingdom, Schonland in

---

16. Pierce, E.T. (1955) Quart. J. Roy. Meteorol. Soc. 81:211-228.
17. MacKerras, D. (1968) J. Geophys. Res. 73:1175-1183.
18. Takeuti, T. (1965) Proc. Res. Inst. Atmos., Nagoya University, 12A:1-70.
19. Workman, E.G., Brook, M., and Kitagawa, N. (1960) J. Geophys. Res. 65:1513-1517.
20. Pierce, E.T. (1970) J. Appl. Meteor. 9:194-195.
21. Smith, L.G. (1957) Quart. J. Roy. Meteor. Soc. 83:103-111.
22. Ogawa, T., and Brook, M. (1964) J. Geophys. Res. 69:5141-5150.
23. Takagi, M. (1961) Proc. Res. Inst. Atmos., Nagoya University, 8B:1-105.
24. Moyer, V.E. (1974) Personal communication.
25. Popov, A.S. (1896) J. Russ. Phys. Chem. Soc. 28:7-9.

South Africa, Bureau in France, Lugeon in Switzerland, Austin in the United States, and Norinder in Sweden.

A common method used to study sferics is the examination of the amplitude frequency spectrum of the received sferic waveform. A broadband receiver may be used to record incident sferic waveforms for analysis. By using electromagnetic propagation laws for very low frequency (VLF), one may make inferences concerning the amplitude spectrum of the source from a study of the received spectrum.[14]

Leushin[26] studied the geographic correspondence of centers of sferic activity and thunderstorms in the Soviet Union and concluded that there is a one-to-one correspondence between them. Barkalova[27] found that there was a good correlation (ranging from 0.73 to 0.97) between the number of thunderstorms and the count of sferics (recorded above a threshold) at two stations in the Soviet Union. It should be mentioned that sferics may originate in Sun or the other stars as well as in lightning.[15]

1.2.3 SFERICS IN THE FORM OF DISCRETE PULSES

Sferics, in general, are continuous, electromagnetic phenomena. Cloud-to-ground discharges, or more precisely, the associated return strokes, produce intense energy in the VLF portion of the spectrum. The noise thus produced is of the form of intermittent pulses superimposed on the continuous, background noise.[28, 29, 30, 23] Horner and Bradley[31] report that the transition from essentially discrete pulses to continuous waveforms occurs between 40 and 550 kHz.

The return stroke of the cloud-to-ground discharge also generates significant sferics (K pulses) at VLF that are perhaps one-tenth the magnitude of the largest pulses.[13] Recoil streamers, which occur when a propagating streamer meets a center of charge opposite in sign to the streamer, produce relatively small K pulses. The leader also generates K pulses, but these are very small in magnitude.[14] Although the various types of K pulses are much less intense than the large, discrete, VLF pulses, they are more numerous and must be considered when analyzing received sferics.[32]

---

26. Leushin, N.E. (1964) AFCRL, Contract AF19(628)-3880, Am. Meteor. Soc. Translation.
27. Barkalova, K.N. (1964) AFCRL, Contract AF19(628)3880, Am. Meteor. Soc. Translation.
28. Horner, F. (1958) J. Atmos. Terr. Phys. 13:140-154.
29. Malan, D.J. (1958) Recent Advances in Atmospheric Electricity, Pergamon, New York, 557-563.
30. Kitagawa, N., and Brook, M. (1960) J. Geophys. Res. 65:1927-1931.
31. Horner, F., and Bradley, P.A. (1964) J. Atmos. Terr. Phys. 26:1155-1166.
32. Pierce, E.T. (1973) Personal communication.

The cloud discharge generates quasi-discrete K pulses at VLF that are remarkably similar to those of the cloud-to-ground discharges. The recoil streamer process is thought to cause these pulses.[14] It is clear that the dominant energy at VLF generated by cloud discharges is due to K pulses.[29, 33]

In summary, both cloud-to-ground and cloud discharges generate significant sferics at VLF in the form of quasi-discrete pulses. The largest pulses, associated with cloud-to-ground discharges, are due to the initial and subsequent return strokes. Both the return stroke (cloud-to-ground discharge) and recoil streamer (cloud-to-ground and cloud discharges) produce quasi-discrete K pulses, which are less intense but more numerous than the "main," VLF pulses. The leader stage of a discharge produces sferic pulses at VLF, but these are very weak in magnitude.

1.3 Objective and Scope of Report

The objective of this study was to contribute information on the following aspects of the climatology of thunderstorms and lightning, with special emphasis on their spatial distribution: an estimation of the distribution over much of the Eastern Hemisphere,* thunderstorm days; the number of lightning discharges; the incidence of lightning discharge; and the areal concentration of lightning discharge.

2. THE SFERICS DATA

2.1 Definition and Source

The sferics data which were available for this study are counts of electromagnetic signals (above a threshold intensity) which emanate from lightning discharges. Personnel of the U. S. Air Force collected these data in 1972 from a large network of sferic sensors capable of recording incident sferics on a global basis.

2.2 The Sferics Recorders

Although sophisticated electronically, the recorders are essentially cathode-ray tube direction finders of the type introduced by Watson-Watt in the United Kingdom more than 40 years ago. The recorders, called signal monitors, are passive remote sensors that detect, classify, and record the vertically polarized component of incident sferics. The location on Earth of a sferic is determined by

---

*The Eastern Hemisphere was selected because of the availability of data from that area.

33. Horner, F. (1960) J. Atmos. Terres. Phys. 21:13-25.

the use of three or more stations. The time of arrival at each station is recorded; then the difference in time of arrival between stations is converted to distance by the use of the estimated propagation rate at VLF. Finally, the location or "fix" of the sferic is determined by a straightforward application of spherical trigonometry. Sferics incident upon the antennas are recorded on a selective basis. The criteria for recording a signal are the azimuth of arrival (sectoring), the waveform cycle characteristics, and the relative intensity of the waveform (thresholding). All incident sferics that are recorded have peak energies in the broadband frequency range of 250 Hz to 60 kHz.[34] Most of the energy from VLF sferics is concentrated near 6 kHz.[3]

All sferic waveforms recorded by the signal monitors satisfied the time and half-cycle criteria illustrated in Figure 1. Also in Figure 1 are examples of actual, large-source-strength sferic waveforms taken from a paper by Kalakowsky and Lewis.[35] The waveforms of VLF sferics (at distances greater than about 60 km) are of the form of sinusoidal waves that build to a peak and then decay to zero. The criteria for recording a waveform are that the half-cycle of maximum amplitude must occur within the first 300 μsec of the waveform and that the total waveform trace must be no greater than 1000 μsec in duration. The actual waveforms shown in Figure 1 were recorded simultaneously at Chicopee and Bedford, Massachusetts, which are 68.6 mi apart. These sferics occurred as single events associated, usually, with cold fronts and squall lines, in close proximity to the monitored area. Since these sferics were very large in peak field strength (20 V m^{-1} at 50 nmi minimum), it is not surprising that all of them meet the criteria shown in Figure 1.

2.3 Area of Data Coverage

The area of data coverage for this study is shown in Figure 2. The area of coverage was determined by a combination of simple azimuthal sectoring and system thresholding. The best estimate of the area of data coverage in the mean for 1972 in the Eastern Hemisphere is that area above the "threshold-sector lines" in Figure 2. Data generally were available north of the broken line in Figure 2 for the period January to July and north of the dash-dot line for the period August to December. Although the available data covered much of the world, exclusive of parts of the Americas, only the Eastern Hemisphere was considered.

The threshold intensity, in decibels, at each grid point is a mean estimate of the minimum field strength below which no signal may be recorded. Virtually all

---

34. Bailey, T.W. (1972) Personal communication.

35. Kalakowsky, C.B., and Lewis, E.A. (1966) Physical Science Research Papers, No. 261, AFCRL Project 4603.

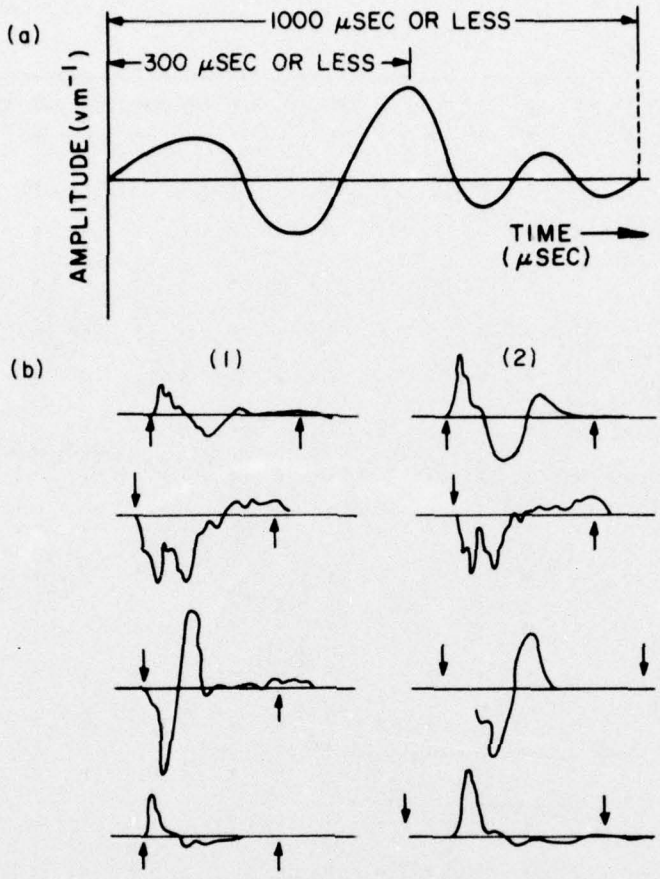

Figure 1. The Time and Half-cycle Criteria (a) for a Sferic Waveform to be Recorded; and Examples (b) of Intense Waveforms Recorded at (1) Chicopee and (2) Bedford, Massachusetts, from the Same Source Thunderstorms. Arrows in (b) are 300 μsec apart and the vertical scale is in V m^{-1}. (After Kalakowsky and Lewis, 1966)

sferics sensors operate above a threshold limit, including the original instrument designed and used by Popov in 1896. The threshold values used in this study were determined by personnel of the U.S. Air Force using a computer-based model. The model inputs were the geographic location of the sensors, propagation laws at VLF, and the individual sensor thresholds (20 dB minimum above a 1 mV m^{-1} reference). The model output was two system threshold arrays (over the grid shown in Figure 2) that give mean threshold values for the periods January to July and August to December of 1972. Sample calculations using these arrays will be presented in Section 3.

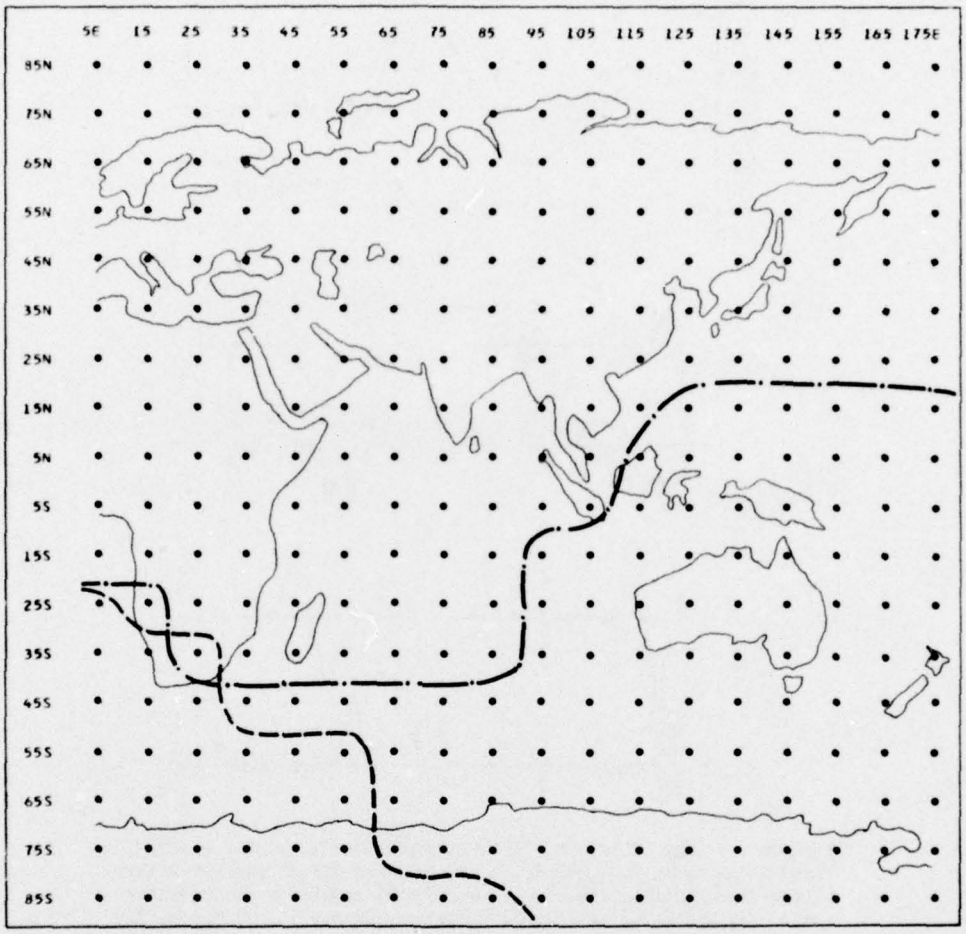

Figure 2. The Area of Data Coverage in the Eastern Hemisphere with Grid Points. Each grid point is centered within a data block bounded by parallels and meridians 10-deg apart. The broken line is an estimate of the threshold-sector line for the period January to July 1972. The dash-dot line is the threshold-sector line for the period August to December 1972. No data were expected south of the threshold-sector lines during the respective periods.

2.4 Aggregation and Volume of Data

There are over 150, 000 datum points (individual counts of signals) available over the Eastern Hemisphere for 1972. The data are aggregated in four synoptic time steps daily (0000-0600Z, 0600-1200Z, 1200-1800Z, 1800-2400Z) and the areal

resolution is by 10-deg latitude and longitude blocks centered about the grid points shown in Figure 2.

A summary of the completeness of the available data, by synoptic time increments, is given in Table 1. Missing data occurred either at random or toward the middle of the month. Therefore, straightforward, linear corrections for missing data were used where necessary.

Table 1. Summary of Number of Calendar Days Data were Available by Synoptic Time Increments for Each Month of 1972 and for the Year

Month	Days	0000-0600Z	0600-1200Z	1200-1800Z	1800-2400Z
Jan.	31	28	28	27	28
Feb.	29	29	29	29	29
Mar.	31	31	31	31	31
Apr.	30	30	30	30	30
May	31	31	31	31	31
June	30	27	27	26	26
July	31	23	24	21	23
Aug.	31	31	31	31	31
Sep.	30	23	23	23	23
Oct.	31	29	30	28	29
Nov.	30	30	30	30	30
Dec.	31	30	30	31	29
Annual	366	342	344	338	340

3. PROCEDURES AND RESULTS OF ANALYSIS

3.1 Thunderstorm Days

An estimate of the number of thunderstorm days at each grid point (with available data) was determined for selected months by simply counting the number of days on which signals occurred. The IBM 360/65 computer of the Data Processing Center was programmed to count the days with signals. A practical constraint was imposed: that the sum of the signals for one day must be at least three in the Northern Hemisphere to be counted. Thus, a zero was entered at those grid points where the sum of the signal count for one day (for example, the sum of the data for 0000-0600Z, 0600-1200Z, 1200-1800Z, 1800-2400Z) was less than three. No similar constraint was imposed for the Southern Hemisphere data.

The reason for the constraint in the Northern Hemisphere was that north of the equator the threshold values were sufficiently low allowing several spurious and erroneous signals to be recorded. An important feature of the system threshold arrays was that relatively few signals were "masked out" in north latitudes, but many signals were masked in south latitudes. In fact, any signal recorded in high south latitudes (say, poleward of 45S) was of relatively great field strength and certainly of thunderstorm origin.[34] The effect of thresholding will be illustrated further in sample calculations in this section.

The mean, global, thunderstorm-day chart of the WMO for January,* is presented in Figure 3. The analyzed results of this study for January are presented in Figure 4. It must be recalled that the results of this study are for the Eastern Hemisphere only. Similar charts are presented for the other classic, climatologic months of April, July, and October. In each of the charts produced in this study, there appears a heavy, dash-dot line (threshold-sector line) which delineates the line south of which the combination of azimuthal sectoring and field-intensity thresholding should have caused a data void. Again, recall that the threshold estimates were averaged over two periods: January to July and August to December, 1972. Therefore, the extent to which the January results in Figure 4 were available "south of the line" may have been a qualitative estimate of the closeness of the actual January data coverage to the estimate in the mean for the period January to July. On the other hand, the amount of data below the line may give an indication of the sensitivity of thresholding. That is, if one assumes that the average threshold array for the period January to July was very close to that for January and that the estimate of azimuthal sectoring was accurate, the degree of "spillover" south of the line gives a feel for the error in the threshold array estimate.

It is very likely that the spill-over effect is due to a combination of the causes outlined in the foregoing paragraph. Regardless of the cause or causes of spillover, it was clear that the recorded data were valid; the problem arises in their treatment.

For the present purpose of estimating the thunderstorm-day distribution for selected months, the spill-over problem is not very significant, because the analysis involves only the counting of signals. However, the problem of spillover becomes important later in this section. The results which appear below the threshold-sector line are counts of days on which intense VLF signals due to lightning discharges (namely, thunderstorms) were recorded. The only ambiguity arises at grid points below the threshold-sector line where blank spaces occur. Here one does not know whether this marks a true data void (that is, no signal occurred), or

---

*Reproduced from the Handbook of Geophysics for Air Force Designers (1960).

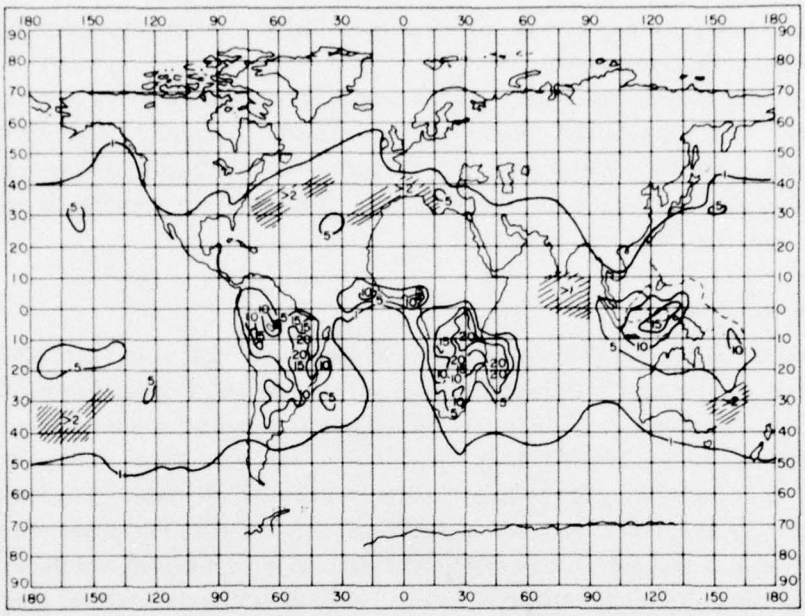

Figure 3. Thunderstorm-day Chart of the WMO for January (all years of record) for the World. Isolines are in thunderstorm days. (After Handbook of Geophysics, 1960)

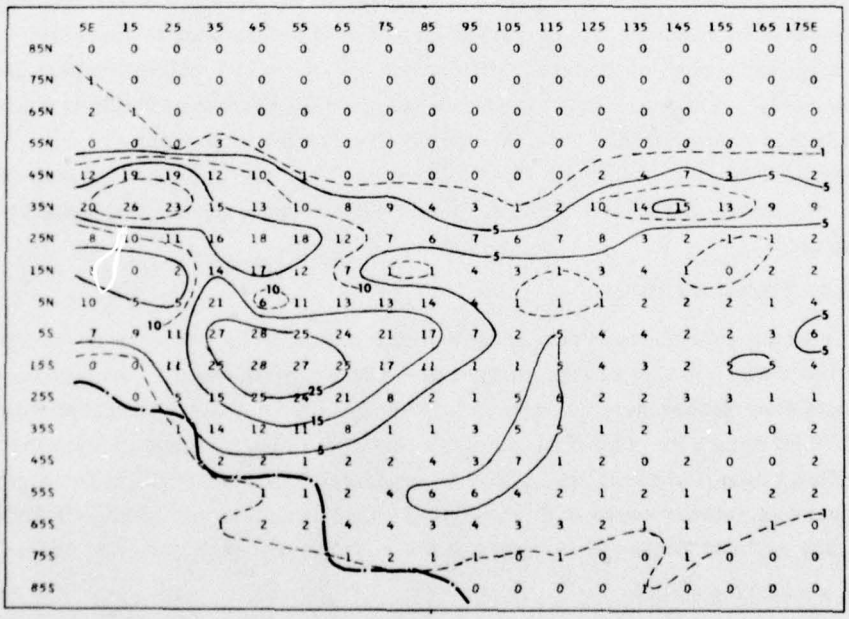

Figure 4. Thunderstorm-day Chart of this Study for January 1972 for the Eastern Hemisphere. The dash-dot line is the average, threshold-sector line for the period January to July 1972. Full isolines are in thunderstorm days. Broken lines are intermediate isolines

the effects of thresholding and sectoring in combination, eliminating signals produced by lightning discharges.

The major thunderstorm areas in the world, as determined by a review of the WMO data,[6] are in North and South America, in West, Central, and South Africa, and in Southeast Asia. These areas are hereafter termed thunderstorm foci because they dominate the world distribution of thunderstorm occurrence on a monthly, seasonal, and yearly basis.

3.2 Evaluation of Results

When comparing the WMO thunderstorm-day charts to those of this study, one should keep in mind that both have inherent advantages and disadvantages. The primary strength of the former is that they cover extensive periods of record at many stations. The years of record vary widely, however, from a low of 1 yr at Agedabia in Africa (30N, 20E) to 52 yr at Ufa in Russia (54N, 45E). The main weaknesses of the WMO effort, as cited in Section 1, are the limitations associated with the observational technique (the hearing and recording of thunder) and the extensive areas over the globe that are void of data. The very low occurrence of thunderstorm activity over the oceans, reflected in the WMO compilation, probably is due to the lack of observations.

The data of this study are internally complete in the spatial dimension, but cover only 1 yr of record. The vagaries intrinsic in the sensing of transient sferics may lead one to question the efficacy of the observational techniques used here. However, it appears that the remote sensing of transient sferics is a more sound observational approach than the human observation of thunder.

A comparison of results with those of the WMO for the month of January can be made by looking at Figures 3 and 4. Some salient observations, by geographic areas, are:

3.2.1 SOUTH AFRICA

The correspondence is close, in order of magnitude, between the South African focus of the WMO and that of this study. The WMO central value of 25 thunderstorm days over Madagascar (15S, 45E) in Figure 3, is in close agreement with the value of 28 in Figure 4. The WMO isolines terminate sharply east of Madagascar in the Indian Ocean, whereas the smoothed analysis of this study indicates a gradual decrease of activity eastward, stretching across the ocean to India. In both studies, the activity decreases sharply at the southern tip of Africa (ca. 35S).

3.2.2 WEST AFRICA

Again, there is agreement in the order of magnitude at the West African focus of thunderstorm days between the two studies. The value of this study in Figure 4 at 5N, 5E of ten thunderstorm days is close to the isoline of ten in the WMO chart.

Both results show a drop in activity to the immediate north. The WMO chart shows a central value of 15, whereas the maximum value of this study is ten in West Africa.

3.2.3 NORTH AFRICA, THE MEDITERRANEAN SEA, AND ARABIA

There are no thunderstorm days shown for January over North Africa in the WMO compilation in Figure 3. A range from zero to 11 thunderstorm days is indicated by this analysis in Figure 4 for the same area (that is, roughly from 15N to 30N latitude in Africa). The central value in the Mediterranean of five in the WMO chart is also much less than the very high value produced in this study of 26 days (35N, 15E) with at least one thunderstorm. The most remarkable difference that shows up consistently is the estimated number of thunderstorm days over Arabia. The WMO shows no thunderstorm days for January in Figure 3, whereas this study shows a central value of 18 at 25N, 45E in Figure 4.

3.2.4 CONTINENTAL EURASIA

In general, the estimates of thunderstorm days produced herein are higher across Eurasia than those of the WMO. Both results show a near paucity of thunderstorms in high latitudes of Eurasia for January. By following the isoline of one thunderstorm day in the Northern Hemisphere in both charts, one may observe that, especially in Eastern Eurasia, the results of this study indicate thunderstorm occurrence much farther poleward than does the WMO.

3.2.5 INDIA

The estimates of the WMO and this study of one or more thunderstorm days in Central and Southern India are in close agreement. As mentioned earlier, the results of this study indicate high thunderstorm activity in the Indian Ocean south of Ceylon, whereas the compilation in the mean of the WMO shows no days with thunderstorms south of 5S. The WMO value of one thunderstorm day in Northern India (for example, at Cherranpunji, approximately 25N, 91E) differs from the estimate of this study of from six to seven thunderstorm days in India along 25N latitude in the foothills of the Himalayas.

3.2.6 JAPAN

A well-defined center of thunderstorm days of 15 off the east coast of Japan (35N, 145E) is estimated herein for January, whereas the WMO chart, shown in Figure 3, indicates only one to five thunderstorm days. There are no thunderstorm days in January over Kyushu, Japan, in the Yellow Sea, or in Korea in the mean, according to the WMO, whereas in this study it is estimated that there are 14 days at 35N, 135E and 10 days at 35N, 125E. Moreover, the estimate of nine thunderstorm days in the North Pacific Ocean along 35N latitude produced in this study is much higher than the estimate of one thunderstorm day reported by the WMO.

3.2.7 SOUTHEAST ASIA

There is no generally accepted delineation of the area that encompasses Southeast Asia. For purposes of discussion, the Southeast Asian focus of thunderstorm days will be defined arbitrarily to include the area bounded by 20N and 10S and 90E and 175E. The estimate in this study of one thunderstorm day for January in the Vietnam area (15N, 115E) shown in Figure 4, agrees with that of the WMO shown in Figure 3. However, the estimate of from four to five thunderstorm days in the East Indies (for example, at 5S, 115E) is much lower than the WMO estimate of 15 thunderstorm days. The well-defined isoline of five thunderstorm days of this study shown in Figure 4 penetrates southward from the East Indies into the Indian and even Southern Ocean area. The isoline of five thunderstorm days of the WMO does not penetrate southward of about 15S latitude in the Indian Ocean.

3.2.8 AUSTRALIA

There is close agreement in the vicinity of Australia between the results for January of the WMO effort and this study. The WMO value of five thunderstorm days across northern Australia (Figure 3) compares well with the values given in this study (Figure 4), ranging from two to five thunderstorm days (that is, along 15S latitude and bounded by 115E and 155E longitude). The value of roughly five thunderstorm days in the area of the Ellice Islands (ca 5S, 175E) also agrees closely with that of the WMO.

3.2.9 ANTARCTICA AND THE SOUTHERN OCEAN

The compilation of the WMO for January shown in Figure 3 indicates no thunderstorm days south of 50S. In this study, VLF signals of the type which emanate from lightning discharges were recorded on at least one day in January throughout much of the Indian and Southern Oceans and even in Antarctica, as shown in Figure 4.

The WMO compilations of thunderstorm days for April (Figure 5), July (Figure 7), and October (Figure 9) were compared to the respective estimates of this study (Figures 6, 8, and 10) in a manner analogous to that given above for January. A comparison between charts by classes of "five thunderstorm days" (that is, 0-5, 5-10, 10-15, and on on) gave a criterion for correspondence. The correspondence was considered "good" if values were within a class in both charts, "fair" if no more than one class apart, and "poor" if more than one class apart. A summary of these comparisons, including that for January, is given in Tables 2 through 5.

The isoline patterns of the WMO charts and those of this study differ markedly. This is not surprising in view of the coarse, grid mesh of this study (that is, values by 10-deg blocks of latitude and longitude) and the concomitant smoothed analyses,

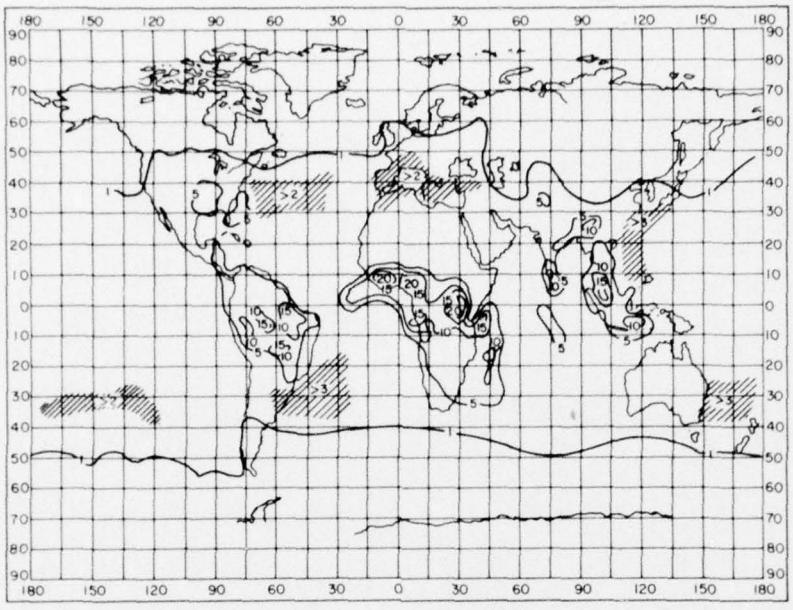

Figure 5. Thunderstorm-day Chart of the WMO for April (all years of record) for the World. Isolines are in thunderstorm days. (After Handbook of Geophysics, 1960)

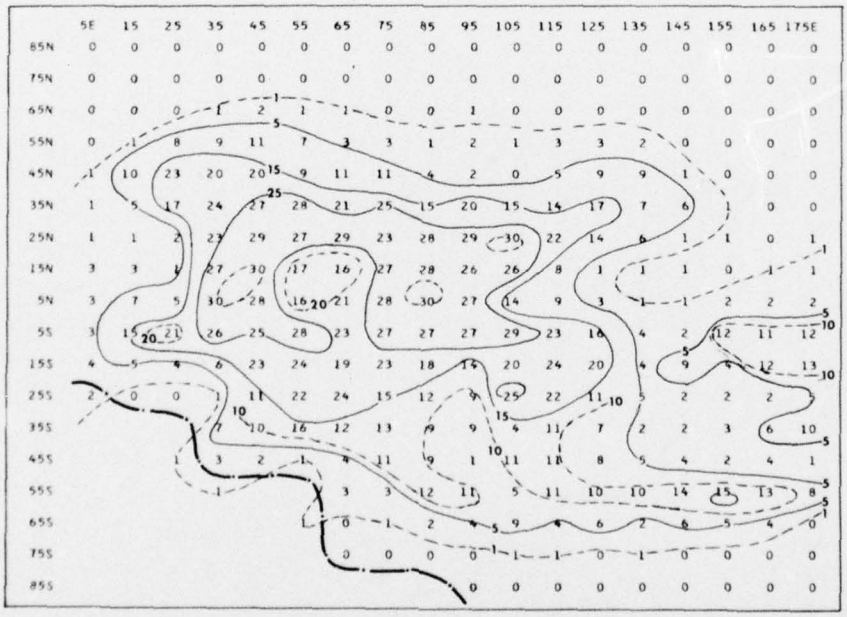

Figure 6. Thunderstorm-day Chart of this Study for April 1972 for the Eastern Hemisphere. The dash-dot line is the average, threshold-sector line for the period January to July 1972. Full isolines are in thunderstorm days. Broken lines are intermediate isolines

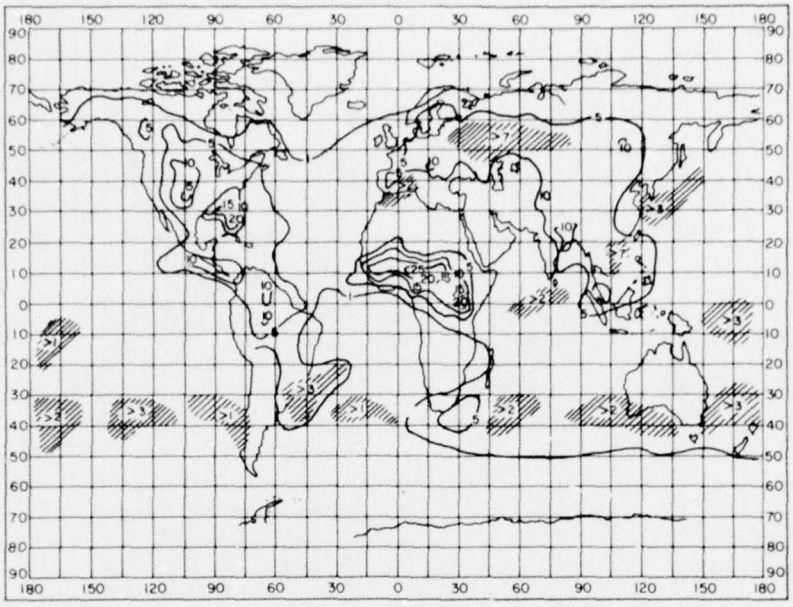

Figure 7. Thunderstorm-day Chart of the WMO for July (all years of record) for the World. Isolines are in thunderstorm days. (After Handbook of Geophysics, 1960)

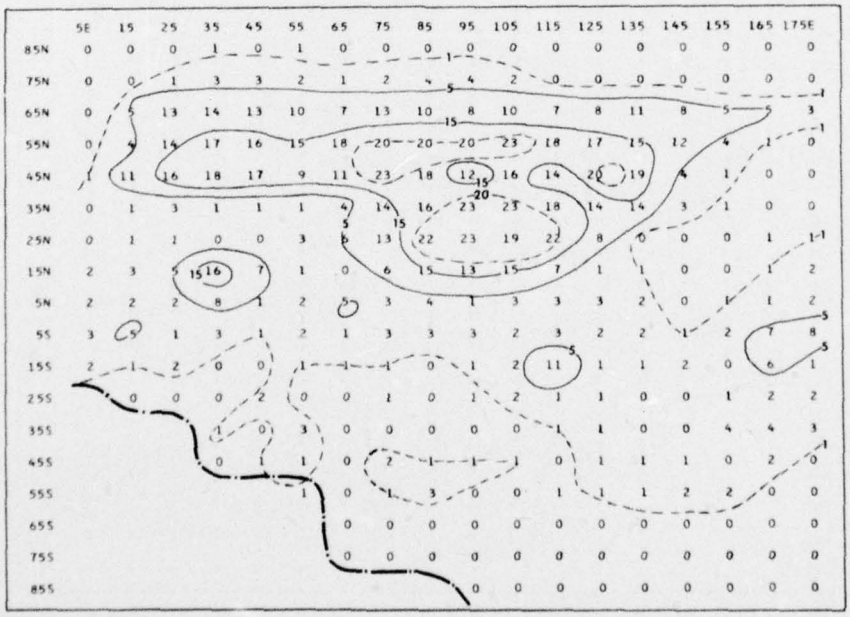

Figure 8. Thunderstorm-day Chart of this Study for July 1972 for the Eastern Hemisphere. The dash-dot line is the average, threshold-sector line for the period January to July 1972. Full isolines are in thunderstorm days. Broken lines are intermediate isolines

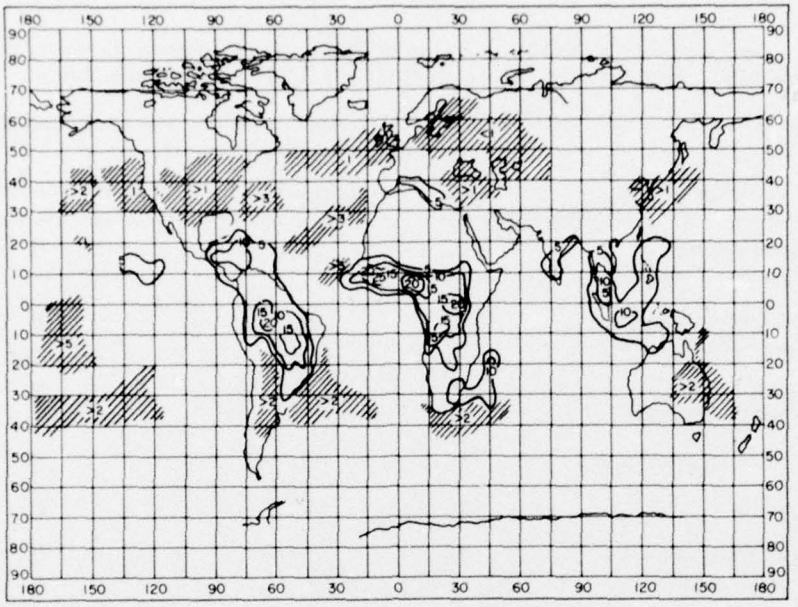

Figure 9. Thunderstorm-day Chart of the WMO for October (all years of record) for the World. Isolines are in thunderstorm days. (After Handbook of Geophysics, 1960)

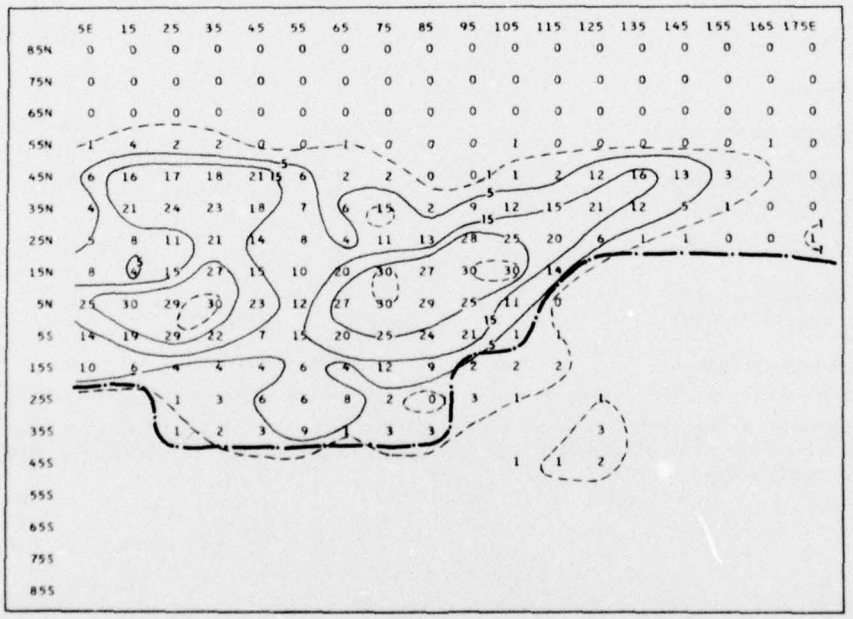

Figure 10. Thunderstorm-day Chart of this Study for October 1972 for the Eastern Hemisphere. The dash-dot line is the average, threshold-sector line for the period August to December 1972. Full isolines are in thunderstorm days. Broken lines are intermediate isolines

Table 2. Comparison of the Compilation of Mean Thunderstorm Days by the WMO over the Eastern Hemisphere for January and the Estimate of this Study*

Area	Typical Value (or Range) WMO	This Study	Correspondence
1. South Africa (south of equator)	25	28	G
2. West and Central Africa	15	10	F
3. North Africa (north of 15N)	0	0-11	P
4. Mediterranean Sea	5	20	P
5. Arabia	0	18	P
6. North Eurasia (north of 35N)	0	0-1	G
7. South Eurasia	1	6	F
8. North India (north of 15N)	1	7	F
9. South India	1	1	G
10. Japan	1	14	P
11. Southeast Asia	15	5	P
12. North Australia (north of 25S)	5	4	G
13. South Australia	1	1	G
14. Indian Ocean (north of 45S)	1	1-17	P
15. Southern Ocean	0	1-6	P

*A judgment of the correspondence in magnitude of the estimates is given as Good (G), Fair (F), or Poor (P) as explained in the text. The isoline patterns differ markedly.

Table 3. Comparison of the Compilation of Mean Thunderstorm Days by the WMO over the Eastern Hemisphere for April and the Estimate of this Study*

Area	Typical Value (or Range) WMO	This Study	Correspondence
1. South Africa (south of equator)	20	21	G
2. West and Central Africa	20	7	P
3. North Africa (north of 15N)	0, >2	1-5	G
4. Mediterranean Sea	>2	5	G
5. Arabia	0	27	P
6. North Eurasia (north of 35N)	1	1-11	P
7. South Eurasia	1-10	20	P
8. North India (north of 15N)	5	28	P
9. South India	5	27	P
10. Japan	1	7	F
11. Southeast Asia	5-15	1-29	F
12. North Australia (north of 25S)	1-5	2-24	P
13. South Australia	1-5	2-22	P
14. Indian Ocean (north of 45S)	1-5	9-24	P
15. Southern Ocean	0-1	1-15	P

*A judgment of the correspondence in magnitude of the estimates is given as Good (G), Fair (F), or Poor (P) as explained in the text. The isoline patterns differ markedly.

Table 4. Comparison of the Compilation of Mean Thunderstorm Days by the WMO over the Eastern Hemisphere for July and the Estimate of this Study*

Area	Typical Value (or Range) WMO	This Study	Correspondence
1. South Africa (south of equator)	1-5	1-5	G
2. West and Central Africa	10-25	2-16	F
3. North Africa (north of 15N)	0-5	0-3	G
4. Mediterranean Sea	0, >2	18	P
5. Arabia	0	0-7	F
6. North Eurasia (north of 35N)	1-10	1-23	P
7. South Eurasia	5-10	23	P
8. North India (north of 15N)	5-10	13	F
9. South India	0-5	6	G
10. Japan	5	14	P
11. Southeast Asia	5-10	0-15	F
12. North Australia (north of 25S)	1-5	0-5	G
13. South Australia	0, >3	0-4	G
14. Indian Ocean (north of 45S)	0, >2	0-3	G
15. Southern Ocean	0-1	0-3	G

*A judgment of the correspondence in magnitude of the estimates is given as Good (G), Fair (F), or Poor (P) as explained in the text. The isoline patterns differ markedly.

Table 5. Comparison of the Compilation of Mean Thunderstorm Days by the WMO over the Eastern Hemisphere for October and the Estimate of this Study*

Area	Typical Value (or Range) WMO	This Study	Correspondence
1. South Africa (south of equator)	5-15	6-29	P
2. West and Central Africa	5-25	8-30	G
3. North Africa (north of 15N)	0-5	8-24	P
4. Mediterranean Sea	5	21	P
5. Arabia	0	14	P
6. North Eurasia (north of 35N)	0-1	1-21	P
7. South Eurasia	0, >1	12	P
8. North India (north of 15N)	5	11	F
9. South India	5	30	P
10. Japan	1	12	P
11. Southeast Asia	5-10	1-30	P

*A judgment of the correspondence in magnitude of the estimates is given as Good (G), Fair (F), or Poor (P) as explained in the text. The isoline patterns differ markedly.

together with the extensive areas of data void in the WMO compilation. There also were wide differences in the point estimates of thunderstorm days. There is generally good agreement in the comparison of the results for the thunderstorm-day focus of South Africa and extremely poor agreement in Arabia. There were 16 good, 10 fair, and 30 poor correspondences of estimates shown in Tables 2 through 5.

One could ascribe various reasons for the differences in correspondence in thunderstorm days between the two studies. An obvious one is that the spatial and temporal differences lead one to expect large differences in results. However, marked differences in thunderstorm days at a station may occur from one year to the next, due to many factors, including the vagaries of the monsoon regime.

Ramage[36] delineates the monsoon area as that between 35N and 25S and between 30W and 170E. He refers to a "bewilderingly complex" pattern of vertical motion throughout the area and states that thunderstorms typically occur rather sporadically during breaks in the steady regime of rain. Outside of the area influenced by the monsoons, there also were considerable differences in correspondence of thunderstorm days between the two studies. It seems likely that many of the differences between the two studies as outlined herein are to be attributed to differences in the respective space and time considerations of the observational techniques.

If one assumes that 1972 was not an anomalous year, then it is clear that the great difference in the estimate of thunderstorm days for Arabia is due either to the lack of meteorological stations in Arabia (leading to a data void in the WMO data) or to the conclusion that the sferics recording system produced erroneous counts of signals. There was only one station (at Hail, 27N, 42E) interior to Saudia Arabia as of 1953 (WMO, 1953). The other 11 stations in Saudia Arabia were either on the coast or on adjacent islands. Griffiths,[37] based on years of experience in Arabia, stated that thunderstorms may occur in the Yemeni Highlands in Southwest Arabia when the low-level flow is northeasterly from the Red Sea or northwesterly from the Mediterranean Sea.

Both thermally induced and frontal thunderstorms are quite possible in desert areas, although the probability of precipitation is slight. An analogy is that it snows quite often in South Texas, but snow rarely reaches the ground as precipitation. The Pacific, Indian, and Southern Oceans are areas where the differences between the two studies in the thunderstorm-day distribution were almost surely due to a lack of data in the WMO compilation.[7]

3.3 The Number of Lightning Discharges

3.3.1 THE PHYSICAL MODEL

In the model employed here, it was assumed that only cloud discharges and cloud-to-ground discharges produce significant, intense, VLF sferics. The model is illustrated in Figure 11.

As described in Section 1, the cloud discharge produces quasi-discrete K pulses in the VLF range of the spectrum. The cloud-to-ground discharge generates the most intense (by an order of magnitude) VLF signals as well as weaker K pulses. The classic cloud model, shown in Figure 11, includes a net, negative center of charge at the height of 3 to 6 km and a net, positive center of charge at a height of 7 to 11 km.[23, 3] Any distribution of charge would be acceptable for the purpose of this study.

36. Ramage, C.S. (1971) Monsoon Meteorology, Academic Press, New York, 296 pp.

37. Griffiths, J.F. (1974) Personal communication.

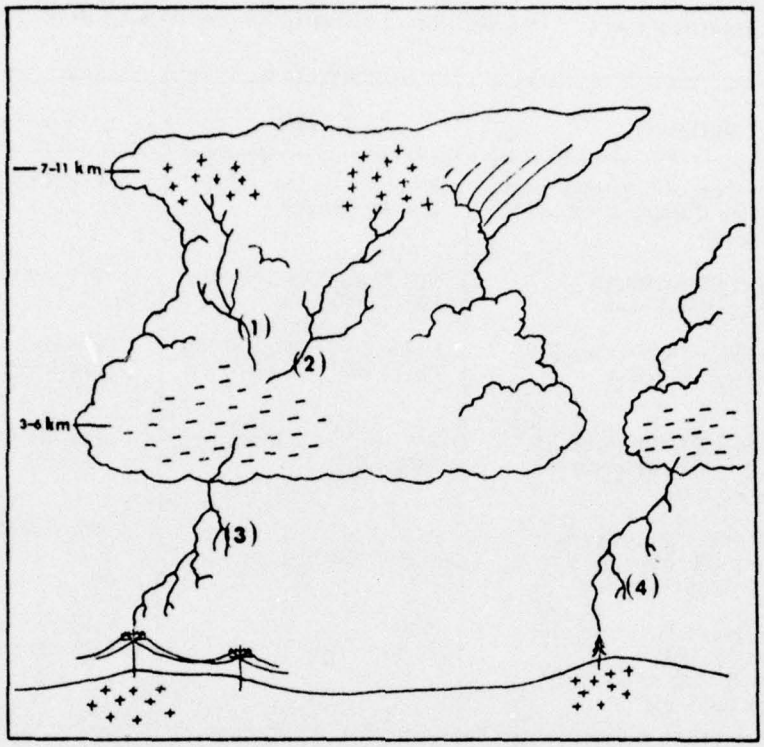

Figure 11. Model of the Thundercloud with Electrical Charge Distribution and Types of Discharge. The latter include cloud discharges (1) and (2) and cloud-to-ground discharges (3) and (4)

3.3.2 THE STATISTICAL DISTRIBUTIONS

The first step in the estimation of the distribution of lightning discharges was to define the appropriate statistical distribution of the received quasi-discrete sferics. Specifically, the distribution of received sferics due to K pulses, the first return stroke, and subsequent return strokes were required. The selection of the appropriate statistics from the literature is presented in Table 6.

There is wide agreement that most parameters of thunderstorm activity follow the log-normal probability law. Horner and Bradley[31] have shown, by an empirical study, that received sferics range in standard deviation from 6 to 8 dB. Pierce[38] states that K pulses due to cloud discharges and those due to cloud-to-ground discharges are remarkably similar in their statistical nature due to the observation

38. Pierce, E.T. (1969) Tech. Rept. 2, SRI Project No. 7045, Contract No. DASA 01-68-C-0073, Stanford Res. Inst., Menlo Park, Calif., 90 pp.

Table 6. Statistics Used to Define Distributions of Sferics Due to Return Strokes and K Pulses

Statistics	Value	Source
Avg. number of K pulses per discharge (cloud or cloud-to-ground)	30 (20-40 range)	Pierce (1969)
Largest field strength intensity of K pulse	0.3 V m^{-1} at 100 km (49.5 dB)	Pierce (1969)
Mean (Med.) field strength intensity of K pulse	0.06 V m^{-1} at 100 km (35.5 dB)	Estimated: ordinary statistical theory
Mean (Med.) field strength intensity of first return stroke sferics	3 V m^{-1} at 100 km (69.5 dB)	Pierce (1973) Horner (1964)
Mean (Med.) field strength intensity of subsequent return stroke sferics	1.5 V m^{-1} at 100 km (63.5 dB)	Pierce (1969)
Standard deviation of field strength intensity of received sferics at very low frequency	7 dB (6 to 8 dB)	Horner and Bradley (1964)

that both types of K pulse are caused by recoil streamers, as explained in Section 1. However, very little is known about K pulses in relation to the more intense types of VLF sferics.

The statistical distributions used in this study were assumed to follow the log-normal law; that is, the peak field strength of all received sferics follow a normal probability distribution about the mean (also the median) with values expressed in decibels namely, on a logarithmic scale. The distributions are defined in Table 7.

The values of field-strength intensity in decibels (dB) given in Table 6 were determined by the following convention:

$$dB = 20 \log \frac{E_p}{E_r} \quad , \tag{1}$$

where E_p is the voltage of the peak received field strength of the waveform above the reference field strength, E_r, of 1 mV m^{-1}. This convention was also used in the threshold array model. The mean field strength value for the K pulse distribution in Table 6 was calculated by assuming, as is frequently done, that the largest

Table 7. Definition of the Statistical Distributions Used in this Study. (Values are in decibels. Standard deviation is denoted by SD)

Sferic Generator	Distribution	Mean	SD	+1 SD	+2 SD	+3 SD
First return stroke	log-normal	69.5	7	76.5	83.5	90.5
Subsequent return strokes	log-normal	63.5	7	70.5	77.5	84.5
K pulses	log-normal	35.5	7	42.5	49.5	56.6

K pulse intensity (field strength of 0.3 V m^{-1}) occurs two standard deviations from the mean. Then, with a standard deviation of 7 dB, one obtains a value of 35.5 dB (or 0.06 V m^{-1}) for the mean intensity by a straightforward application of the normal law.

3.3.3 LATITUDINAL VARIATION OF LIGHTNING PARAMETERS

Pierce[20] gave the only available estimate, based on empirical studies, of the variation with latitude of the average number of return strokes per cloud-to-ground discharge and the proportion of all discharges that go to ground. The line of best fit, based on nine sets of data, for the average number of return strokes per cloud-to-ground discharge, n, has the equation

$$n = 6 - (\phi/30) \quad , \tag{2}$$

where ϕ is latitude in degrees. The equation for the proportion of ground discharges, P, is

$$P = 0.1\,[1 + (\phi/30)^2] \quad , \tag{3}$$

where ϕ is the latitude in degrees. This equation is the best fit for 19 sets of data. As Pierce[20] points out, other factors (orography, type of thunderstorm, and so on) ideally should be considered to refine the "rough fit" represented by these equations.

One may develop[38] from Eq. (3) an expression for the ratio, M, of the number of cloud discharges, D_C, to the number of cloud-to-ground discharges, D_G, for a given latitude, ϕ:

$$M = \frac{D_C}{D_G} \quad . \tag{4}$$

Then

$$M = \frac{9 - (\phi/30)^2}{1 + (\phi/30)^2} \quad . \tag{5}$$

Since, by definition, there is only one first return stroke per cloud-to-ground discharge, it follows from Eq. (2) that the number of subsequent return strokes per discharge, q, for a given latitude, ϕ, may be written

$$q = 5 - (\phi/20) \quad . \tag{6}$$

The relationship, in the mean, among the first return stroke, R_1, the subsequent return strokes, R_S, and K pulses (due to the cloud discharge or cloud-to-ground discharge) is

$$R_1:R_S:K = 1:q:30 \quad , \tag{7}$$

where q is taken from Eq. (6) and the mean value, 30, from Table 6.

A sense of the latitudinal variation of the lightning parameters given by Eqs. (2), (3), (5), and (6) is given in Table 8. With the exception of the proportion of all discharges that go to ground, P, which increases poleward, all parameters in Table 8 decrease in magnitude from equator to pole. Pierce[20] stated that this increase may be explained by a meteorological argument: The smaller the discharge distance in the cloud (that is, from the net, negative center of charge to the net, positive center of charge in Figure 11) relative to the discharge distance from the negative cloud center of charge to the ground, the greater the probability of a cloud discharge relative to a discharge to ground. This concept leads one to infer that the height of the net, negative center of charge is greater on the average in the tropics than in temperate and polar latitudes, although this has not been demonstrated. It should be mentioned that the ratio of cloud to cloud-to-ground discharges, M, was constrained to be no less than unity. It seems most unlikely that there are more ground than cloud discharges, on the average, even at high latitudes.

Table 8. Latitudinal Variation of Lightning Parameters by 5-deg Latitude Increments from Equator to Pole. (The values are applicable in both the Northern and Southern Hemispheres)

Latitude (deg)	n	q	P	M
0	6.00	5.00	0.10	9.00
5	5.75	4.75	0.10	8.73
10	5.50	4.50	0.11	8.00
15	5.25	4.25	0.12	7.00
20	5.00	4.00	0.14	5.92
25	4.75	3.75	0.16	4.90
30	4.50	3.50	0.19	4.00
35	4.25	3.25	0.22	3.24
40	4.00	3.00	0.26	2.60
45	3.75	2.75	0.30	2.08
50	3.50	2.50	0.35	1.65
55	3.25	2.25	0.40	1.29
60	3.00	2.00	0.46	1.00
65	2.75	1.75	0.52	1.00
70	2.50	1.50	0.59	1.00
75	2.25	1.25	0.66	1.00
80	2.00	1.00	0.74	1.00
85	1.75	0.75	0.82	1.00
90	1.50	0.50	0.91	1.00

n Average number of return strokes (first and subsequent) per cloud-to-ground discharge.

q Average number of subsequent return strokes per cloud-to-ground discharge (n-1).

P Proportion of all discharges that go to ground.

M Ratio of the number of cloud discharges to the number of cloud-to-ground discharges.

3.3.4 DETERMINATION OF THE NUMBER OF LIGHTNING DISCHARGES

Two procedures for estimating the number of lightning discharges at each grid point were developed under different assumptions. In the first procedure, Case 1, the assumption was made that the values of threshold intensity were sufficiently large to preclude the sensing of K pulses; that is, it was assumed that only sferics due to the intense return stroke of the cloud-to-ground discharge were recorded by the sferics network. The absolute minimum threshold value in the threshold arrays was 49.4 dB. This value represents that intensity in field strength below which no signal theoretically could have been recorded. All other threshold values were 50 dB or greater. The minimum threshold intensity of 49.4 dB was nearly two standard deviations greater than the mean of the K distribution, as seen from Table 7. Therefore, if the sample statistics given in Table 6 were close approximations to the state-of-nature, and if the threshold values were reasonable estimates of system response in the mean, then, clearly, few K pulses were recorded by the sferics system.

In the second procedure, Case 2, the assumption was made that K pulse sferics were recorded as well as sferics due to return strokes. Case 1 was used in the actual analyses of the data.

In Case 1, we express the number of VLF signals recorded, X, at a given grid point as

$$X = Q_1 R_1 + Q_S R_S \quad , \tag{8}$$

where R_1 is the first return stroke (always one per cloud-to-ground discharge) and R_S is the number of subsequent return strokes per discharge (varies with latitude). The symbols Q_1 and Q_S are the respective probabilities of occurrence of a single R_1 or R_S sferic above a lower limit of threshold intensity.

One may understand better Eq. (8) by the use of relative probability curves.[39] Relative probability, as used here, is defined as the probability of occurrence of a single even (R_1 or R_S) with respect to a reference (for example, the mean, field-strength intensity of the R_1 distribution). The log-normal curves of relative probability for R_1 and R_S that are valid along the equator are shown in Figure 12. (One must construct a different set of curves for each of the 18 latitude points in the grid in Figure 2.) A given threshold intensity serves as the lower limit, in decibels, of the probability integral for a given distribution. For example, in the typical case of a threshold intensity of 53.6 dB at 55N, 35E, the probability of occurrence of a first return stroke greater than or equal to 53.6 dB may be expressed according to the log-normal law as

39. Pierce, E.T. (1968) Tech. Rept. 49, SRI Project No. 4240, Contract No. DA 36-039-AMC-00040E, Stanford Res. Inst., Menlo Park, Calif., 94 pp.

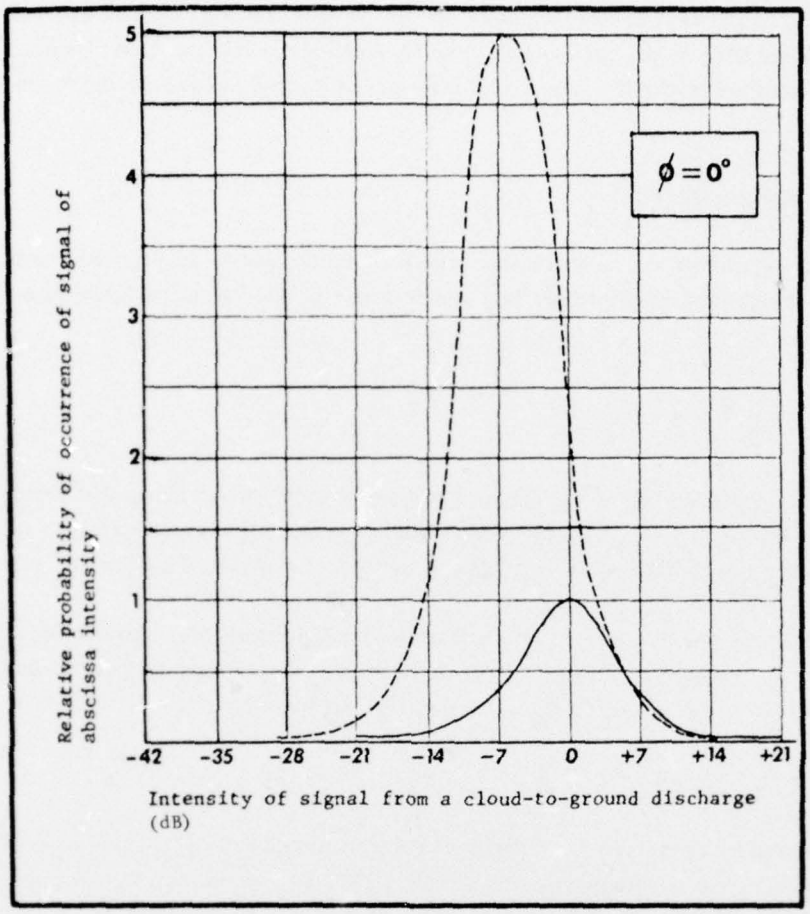

Figure 12. Probability of Occurrence of a Signal above a Threshold Intensity at the Equator Relative to the Mean (set to zero) of First Return Stroke Distribution (solid curve). Broken curve is subsequent return stroke distribution. Latitude is ϕ

$$Q_1 = \frac{1}{\sigma\sqrt{2\pi}} \int_{53.6}^{\infty} \left\{ \exp\left[-\frac{(T - \overline{T})^2}{2\sigma^2} \right] \right\} dT \quad , \tag{9}$$

where σ is the standard deviation (assumed to be 7 dB) and T, in decibels, is the threshold intensity. The curves in Figure 12 were constructed relative to the mean of the first return stroke distribution (set to zero) along the abscissa and in accordance with the proportions given by Eq. (7) for the ordinate values. Abscissa values,

therefore, represent decibel values "up" or "down" the logarithmic scale of intensity relative to the mean of the distribution of the first return stroke.

We may solve for R_S in Eq. (7) in terms of R_1 and substitute for R_S in Eq. (8) to obtain

$$X = Q_1 R_1 + qQ_S R_1 \quad . \tag{10}$$

Then we may solve Eq. (10) for R_1, which is equivalent to solving for the number of cloud-to-ground discharges, D_G, since there is one "first return stroke," R_1, per D_G:

$$D_G = \frac{X}{Q_1 + qQ_S} \quad . \tag{11}$$

Now by the substitution of the appropriate probability integrals in the denominator of Eq. (11), Q_1 and Q_S, with the concomitant value of threshold intensity at a grid point as the lower limit in each integral, we may solve Eq. (11) for D_G at the grid point.

The final step in Case 1 is to find an estimate of the total number of discharges, D_T, comprised of cloud discharges, D_C, and cloud-to-ground discharges, D_G. By the substitution for D_C from Eq. (4) we have

$$D_T = D_G (1 + M) \quad . \tag{12}$$

A sample calculation for Case 1 of the estimated number of lightning discharges, D_T, that occurred during January 1972 within the data block centered on 25N, 125E (1, 119, 165 km^2) is

ϕ = 25N (latitude)

x = 688 (sum of all VLF signals recorded at 25N, 125E for January 1972)

X = 769 (x adjusted for missing data ... the average data coverage for January was 27.75 from Table 1 ... a linear adjustment is (31/27.75) (688) or 768.6 signals)

T = 66.9 dB (threshold value at 25N, 125E which is the lower limit on the probability integrals)

q = 3.75 (number of return strokes per cloud-to-ground discharge at 25N or 25S latitude ... from Table 8)

M = 4.90 (ratio of the number of cloud to cloud-to-ground discharges at 25N or 25S latitude ... from Table 8)

Then the procedure used to obtain Eq. (9) yields a Q_1 of 0.644 and a Q_S of 0.316. (The mean of the first return stroke distribution is 69.5 dB from Table 7. Therefore, the threshold value of 66.9 dB at 25N, 125E is "2.6 dB down" from the mean. One may estimate Q_1 and Q_S by looking at the respective areas under the curves to the right of the -2.6 dB abscissa value in Figure 12). We now may solve Eq. (12) for the estimated number of lightning discharges, D_T, that occurred during January 1972 within the data block centered on 25N, 125E.

$$D_T = \frac{769}{0.644 + (3.75)(0.316)} (1 + 4.9) \quad ,$$

$$= 2480 \quad .$$

This value appears in Figure 13 at 25N, 125E, rounded off to the nearest 100 lightning discharges (that is, 25).

The IBM 360/65 computer was programmed to solve Eq. (12) for the estimated number of lightning discharges, D_T, at each grid point in Figure 2 in the following expanded form

$$D_T = \frac{X}{\frac{1}{\sigma\sqrt{2\pi}}\int_{T_o}^{\infty} \exp\left[-\frac{(T - \overline{T})^2}{2\sigma^2}\right] dT + q\left\{\frac{1}{\sigma\sqrt{2\pi}}\int_{T'_o}^{\infty} \exp\left[-\frac{(T' - \overline{T}')^2}{2\sigma^2}\right] dT'\right\}}$$

$$[1 + M] \quad , \qquad (13)$$

where the unprimed quantities refer to the distribution of the first return stroke and the primed quantities refer to that of the subsequent return stroke; X is the number of VLF signals recorded; σ is the standard deviation (7 dB in both distributions); T_o is the threshold value at a given grid point; $\overline{T}$ is the intensity of the mean (median) field strength of received signals in decibels; q is the number of subsequent return strokes per cloud-to-ground discharge given by Eq. (6); and M is the ratio of cloud to cloud-to-ground discharges given by Eq. (5).

In Case 2, we assume that K pulses, which may originate in both cloud discharges and cloud-to-ground discharges, were recorded by the system. Equation (8) now becomes

$$X = \underbrace{Q_1 R_1 + Q_S R_S + Q_K K_G}_{(1)} + \underbrace{Q_K K_C}_{(2)} \quad . \qquad (14)$$

Term (1) is the contribution due to the cloud-to-ground discharge. The symbols Q_1, Q_S, and Q_K are the probabilities of occurrence of the first return stroke, subsequent return strokes, and K pulses, respectively. We use R_1 and R_S as before, and K_G is the number of recorded K pulses due to the ground discharge. Term (2) is the contribution due to the cloud discharge. Since we assumed that the statistics of K pulses were identical regardless of origin, Q_K is the same as in term (1). The number of recorded K pulses due to the cloud discharge is represented by K_C.

By substitution for R_S, K_G, and K_C in Eq. (14) with their equivalents from Eq. (7), we may solve for the number of cloud-to-ground discharges, D_G (same as R_1), as in Case 1:

$$D_G = \frac{X}{Q_1 + qQ_S + 30Q_K + 30MQ_K} \quad . \tag{15}$$

A sample calculation for Case 2, which is hypothetical since Case 2 was not used in the analysis, is as follows.

Let

ϕ = 65N (latitude)

X = *500 (sum of all VLF signals recorded during* one month at a grid point)

T = 50.0 dB (threshold intensity)

Following the procedure in Case 1, we obtain these values:

Q_1 = 0.99

Q_S = 0.97

Q_K = 0.02

q = 1.75 (from Table 8)

M = 1.00 (from Table 8)

Then Eq. (15) may be solved for the estimated number of lightning discharges, D_T:

$$D_T = \frac{500}{0.99 + (1.75)(0.97) + 30(0.02) + 30(1.0)(0.2)} [1 + 1.0] \quad ,$$

$$= 330 \quad .$$

The result for D_T if we use the initial values given here, but under the Case 1 assumption that no K pulses are recorded, is

$$D_T = (186)(1 + 1.0) = 372 \quad .$$

That is, for a grid point at 65N with an associated threshold intensity of 50.0 dB, the Case 1 procedure leads to an estimate of the number of lightning discharges, roughly 11 percent higher than that for Case 2.

Since the very low threshold intensity of 50.0 dB leads to a difference of only 11 percent between the results of the Case 1 and Case 2 procedures, it was evident that the choice of procedure was not critical to the work as long as the threshold values were valid. If the threshold values were significantly lower, the choice of procedure would have been very critical. As mentioned earlier, the lowest threshold intensity at a grid point was 49.4 dB. All other values were greater than 50.0 dB.

The results of the Case 1 type analysis of the sferics data are given in Figures 13 through 25 for each month in 1972 and for the year as a whole. The background map shown in Figure 2 appears in each of these figures. Smoothed isolines of the grid point results are given in powers of 10 (that is, 10^2 to 10^6), and the chart entries are in hundreds of discharges. The threshold-sector lines that appeared in the thunderstorm-day charts (Figures 6 through 10) were reproduced here for each month. It is to be recalled that this line for a given month is an estimate, based on arrays of mean threshold intensity, that delineates the areal extent of data coverage (north of the line) due to the combination of minimum limits of threshold intensity and azimuthal sectoring.

Values and isolines that appear south of the threshold-sector line should be viewed with extreme caution. The extent to which the values and isolines "spill over" the line may be a measure of the incorrectness of the threshold array itself, or it may simply be a result of individual monthly departures from the mean estimates. Due to the practical problem that no values of threshold intensity were available south of the threshold-sector line, the convention was adopted that the threshold value of the "three-standard-deviation point" of each of the statistical distributions (given in Table 7) was used everywhere south of the line. The prudent decision, in view of all the uncertainties, may be to ignore all results below the threshold-sector line.

It is further recommended that all values that appear at and south of 45S latitude in Figures 13 through 25 be considered questionable until confirmation or rejection of them, based on other studies, is possible. This is due to the fact that values of threshold intensity were very close to the three-standard-deviation point of the respective distributions given in Table 7 at and south of 45S. The result is that only a few recorded signals south of 45S were converted to many discharges by the use of the probability integral technique explained previously. This may

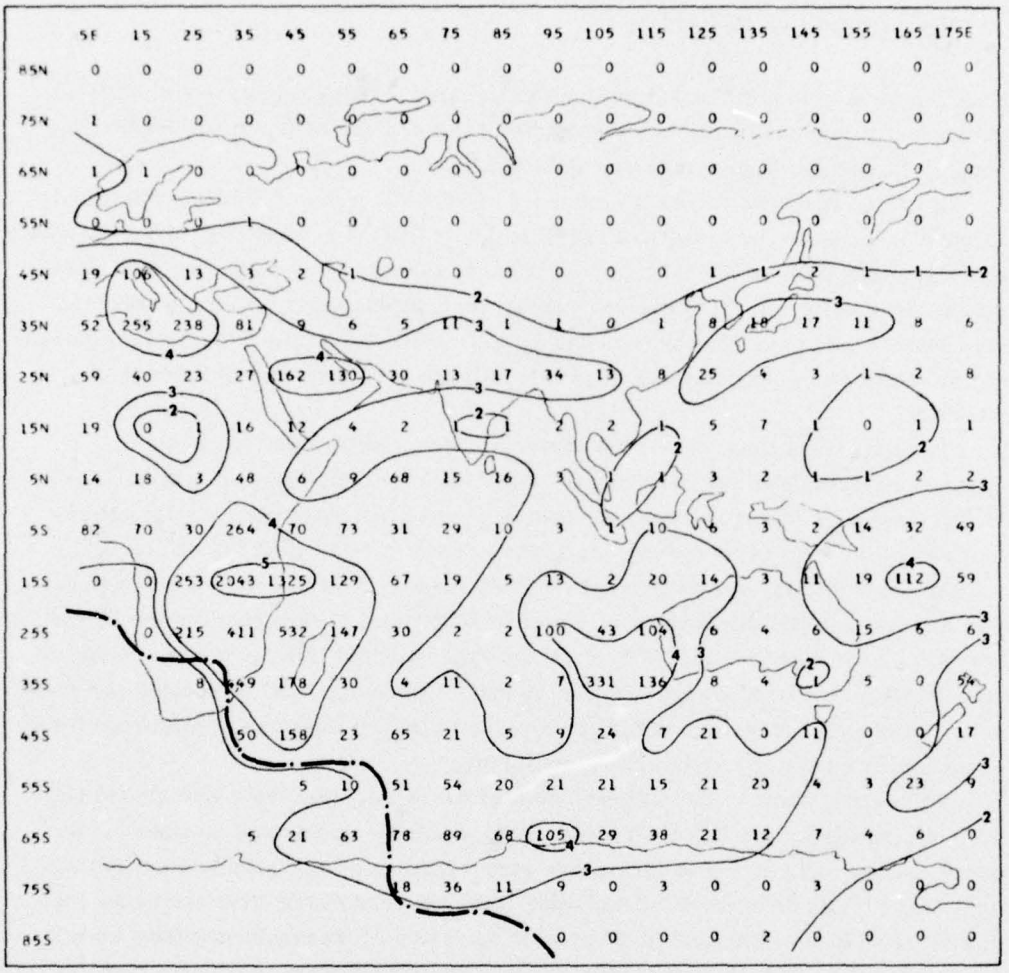

Figure 13. Distribution of the Estimated Number of Lightning Discharges for January 1972. The dash-dot line is the average threshold-sector line for the period January to July 1972. Values are in hundreds of discharges for 10-deg data blocks centered at the points shown. Isolines are number of discharges in powers of 10

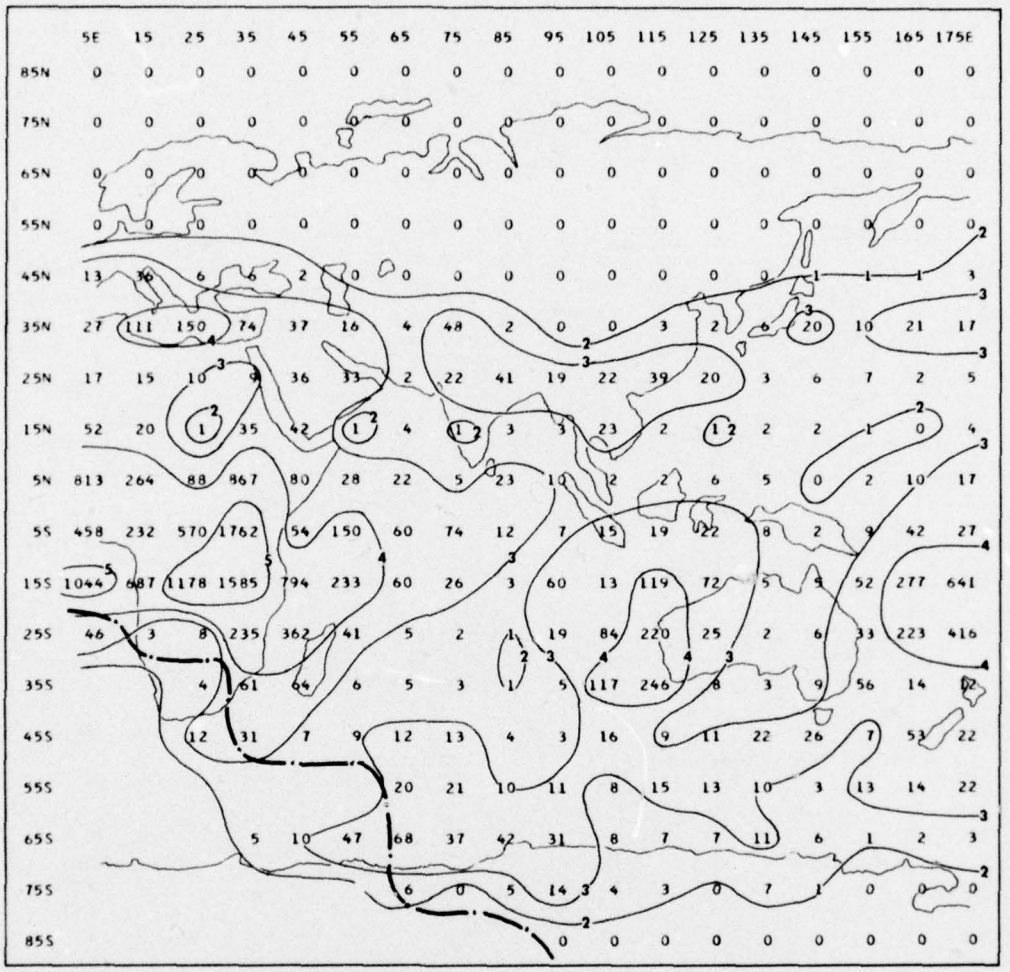

Figure 14. Distribution of the Estimated Number of Lightning Discharges for February 1972. The dash-dot line is the average threshold-sector line for the period January to July 1972. Values are in hundreds of discharges for 10-deg data blocks centered at the points shown. Isolines are number of discharges in powers of 10

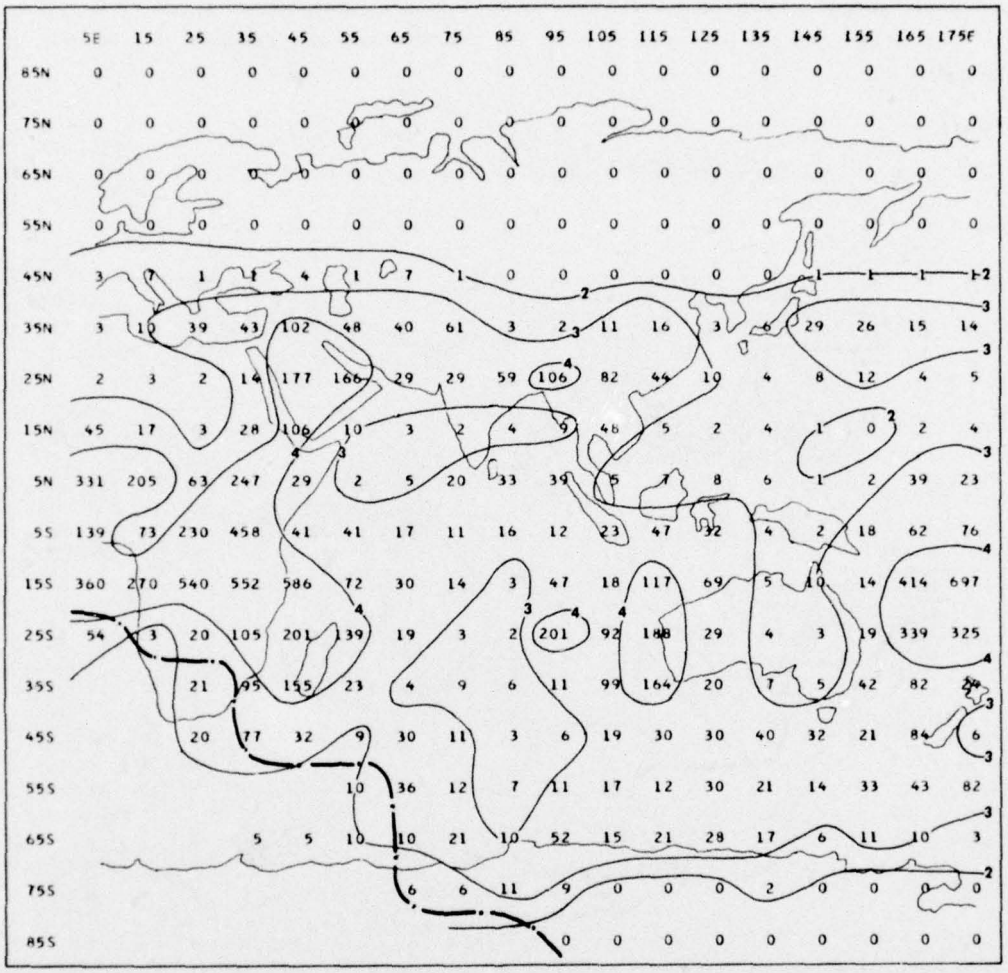

Figure 15. Distribution of the Estimated Number of Lightning Discharges for March 1972. The dash-dot line is the average threshold-sector line for the period January to July 1972. Values are in hundreds of discharges for 10-deg data blocks centered at the points shown. Isolines are number of discharges in powers of 10

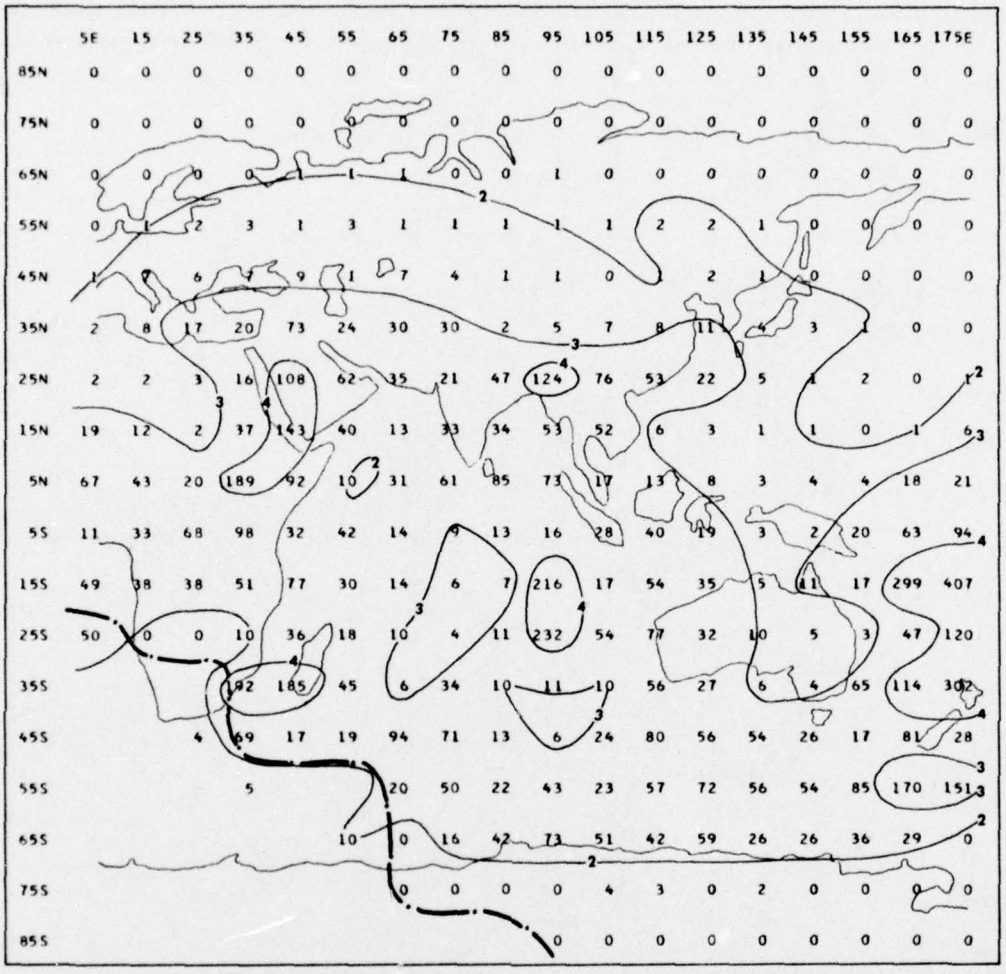

Figure 16. Distribution of the Estimated Number of Lightning Discharges for April 1972. The dash-dot line is the average threshold-sector line for the period January to July 1972. Values are in hundreds of discharges for 10-deg data blocks centered at the points shown. Isolines are number of discharges in powers of 10

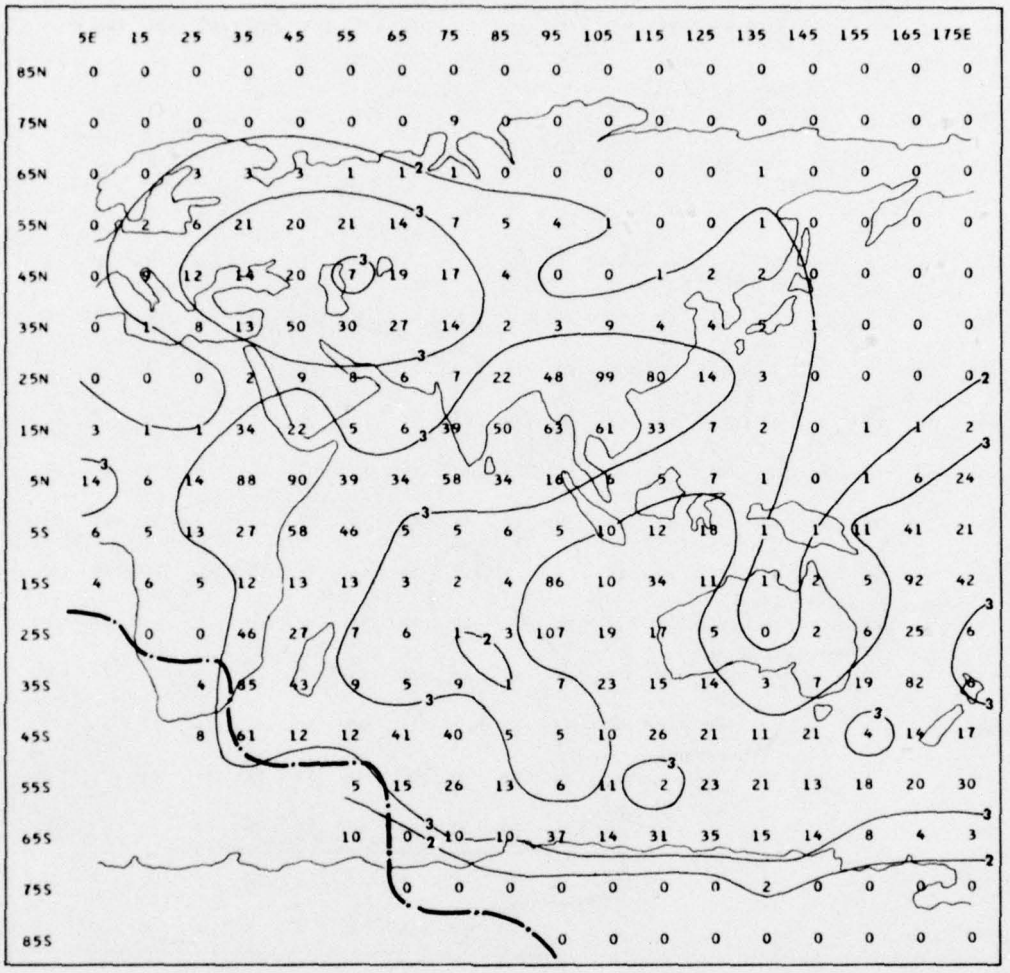

Figure 17. Distribution of the Estimated Number of Lightning Discharges for May 1972. The dash-dot line is the average threshold-sector line for the period January to July 1972. Values are in hundreds of discharges for 10-deg data blocks centered at the points shown. Isolines are number of discharges in powers of 10

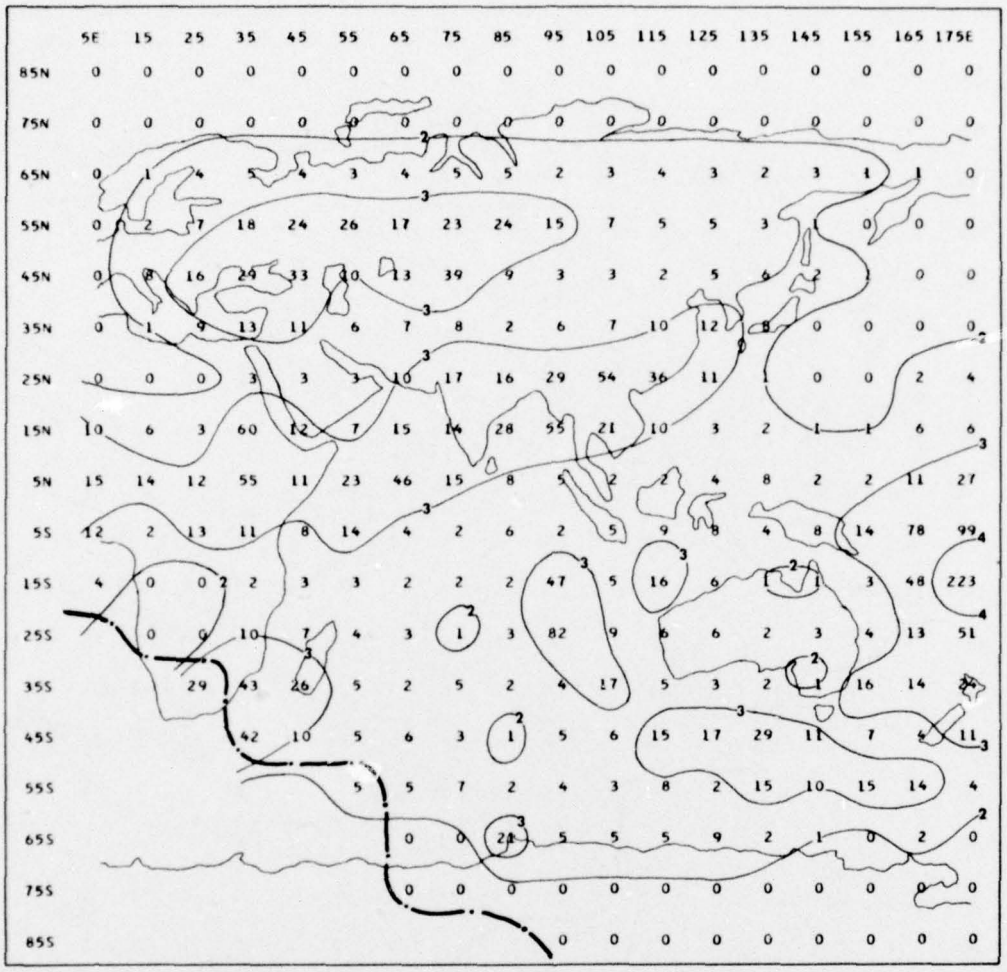

Figure 18. Distribution of the Estimated Number of Lightning Discharges for June 1972. The dash-dot line is the average threshold-sector line for the period January to July 1972. Values are in hundreds of discharges for 10-deg data blocks centered at the points shown. Isolines are number of discharges in powers of 10

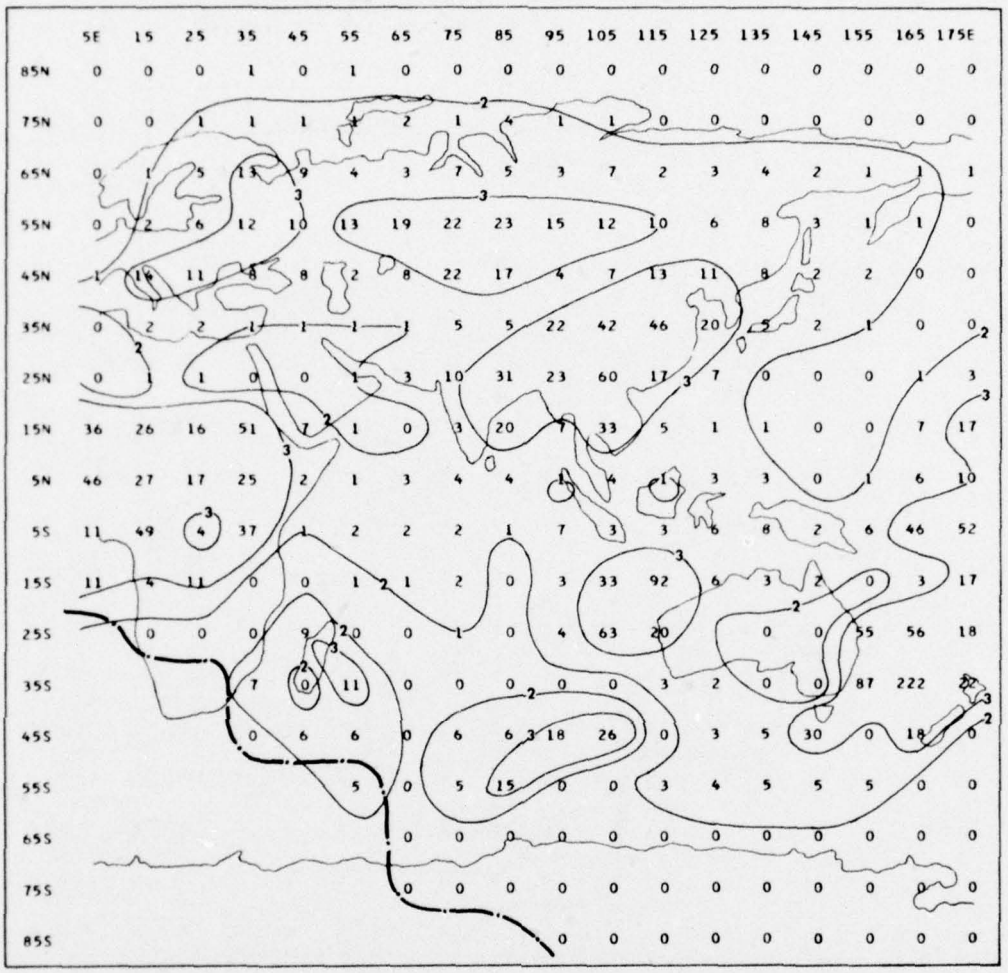

Figure 19. Distribution of the Estimated Number of Lightning Discharges for July 1972. The dash-dot line is the average threshold-sector line for the period January to July 1972. Values are in hundreds of discharges for 10-deg data blocks centered at the points shown. Isolines are number of discharges in powers of 10

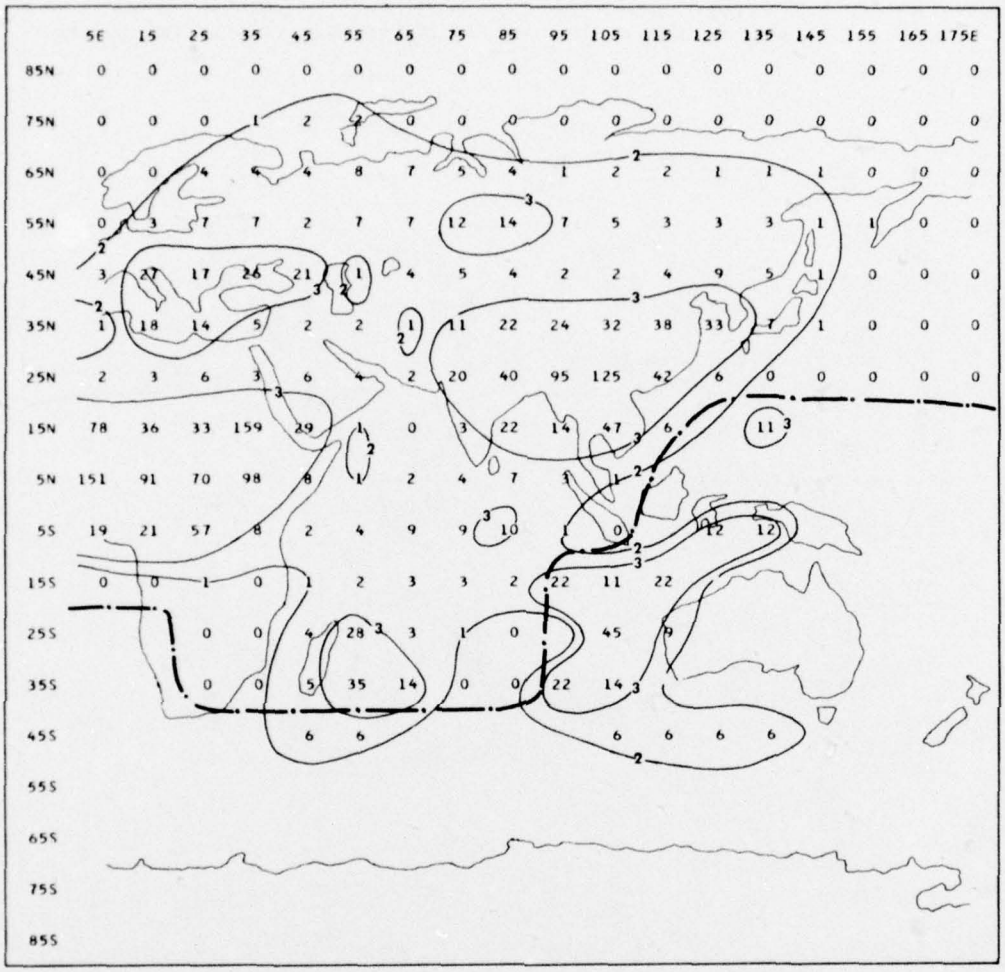

Figure 20. Distribution of the Estimated Number of Lightning Discharges for August 1972. The dash-dot line is the average threshold-sector line for the period August to December 1972. Values are in hundreds of discharges for 10-deg data blocks centered at the points shown. Isolines are number of discharges in powers of 10

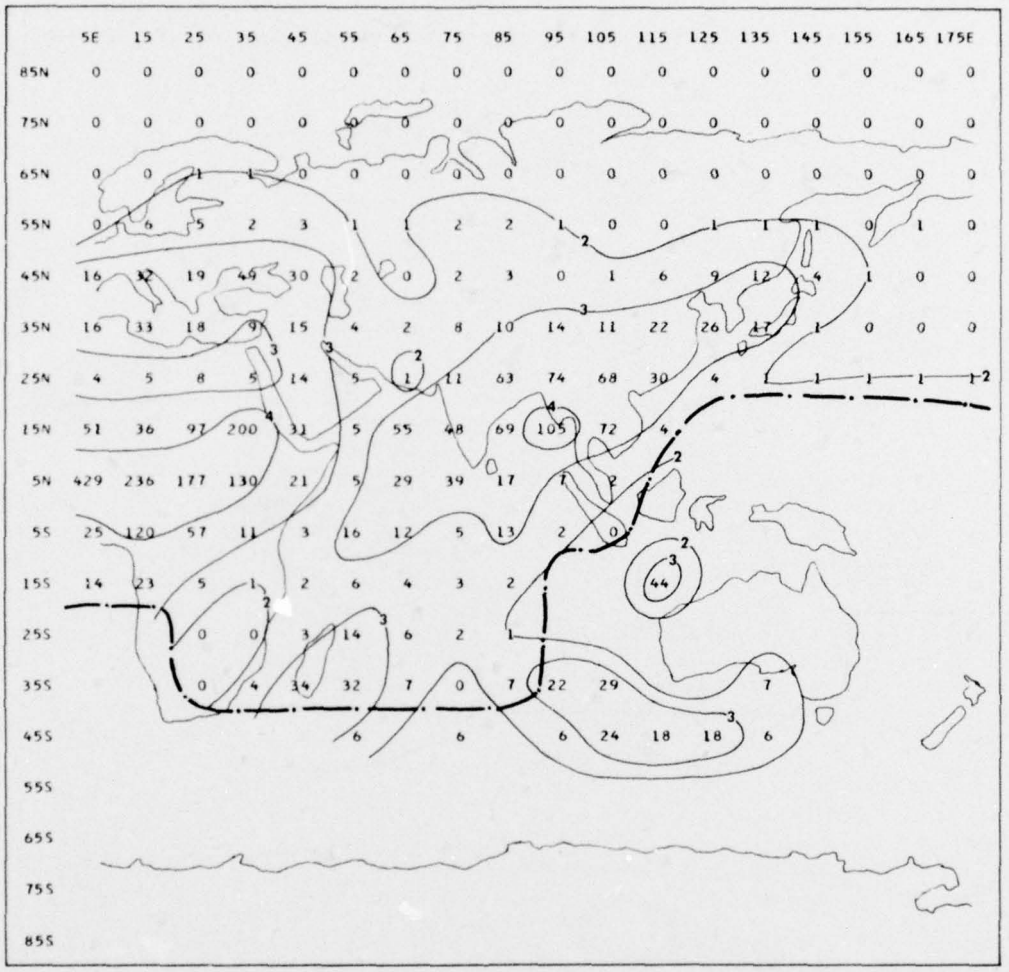

Figure 21. Distribution of the Estimated Number of Lightning Discharges for September 1972. The dash-dot line is the average threshold-sector line for the period August to December 1972. Values are in hundreds of discharges for 10-deg data blocks centered at the points shown. Isolines are number of discharges in powers of 10

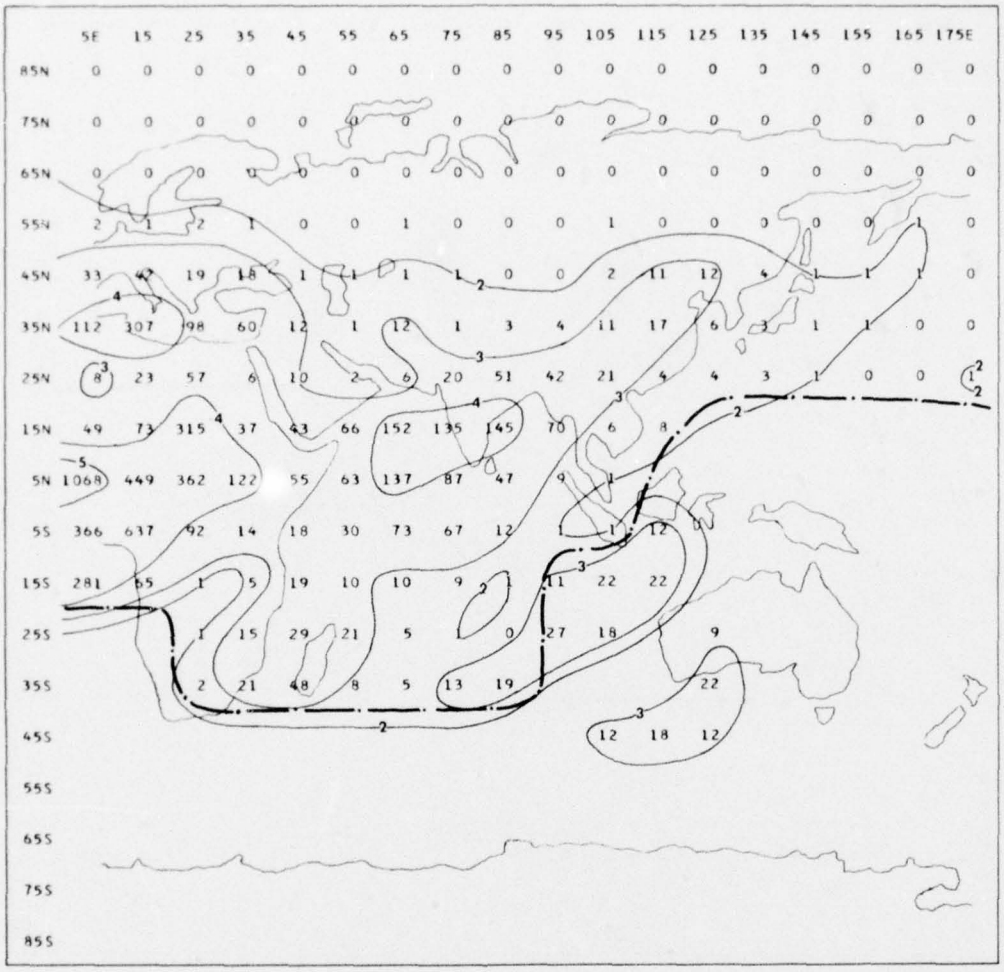

Figure 22. Distribution of the Estimated Number of Lightning Discharges for October 1972. The dash-dot line is the average threshold-sector line for the period August to December 1972. Values are in hundreds of discharges for 10-deg data blocks centered at the points shown. Isolines are number of discharges in powers of 10

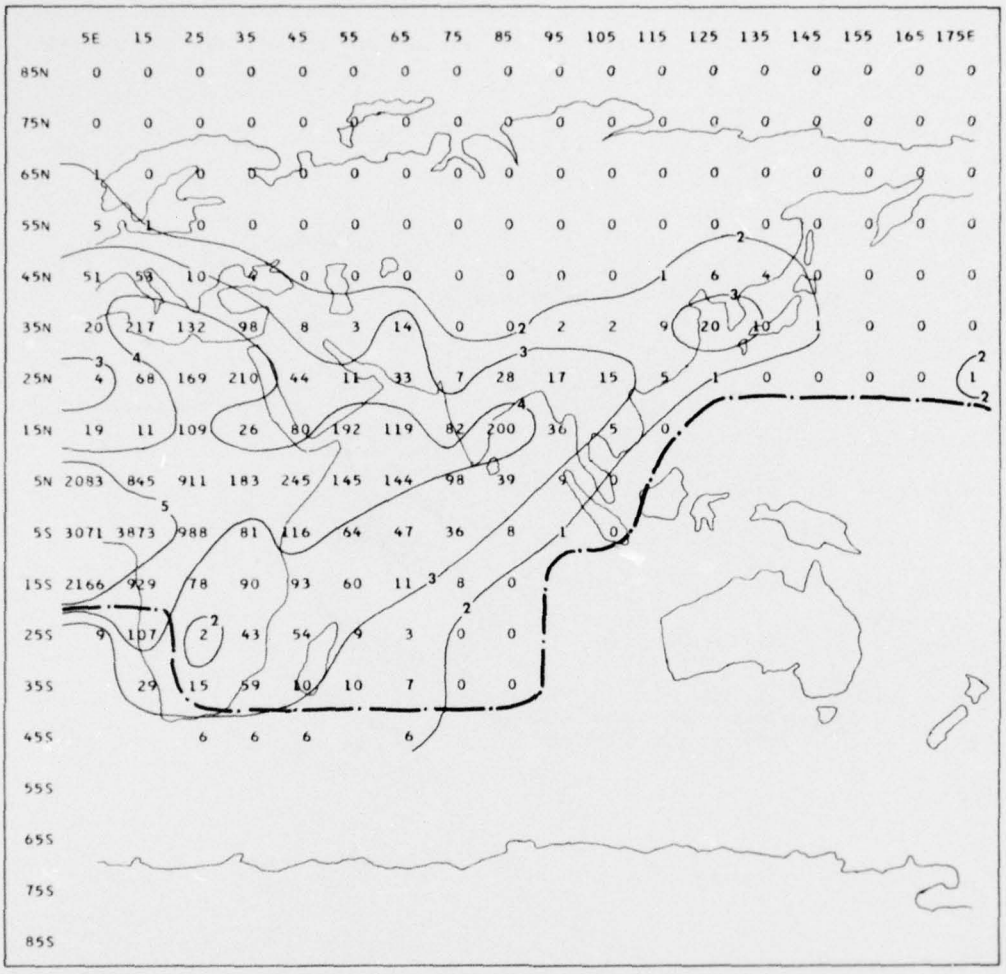

Figure 23. Distribution of the Estimated Number of Lightning Discharges for November 1972. The dash-dot line is the average threshold-sector line for the period August to December 1972. Values are in hundreds of discharges for 10-deg data blocks centered at the points shown. Isolines are number of discharges in powers of 10

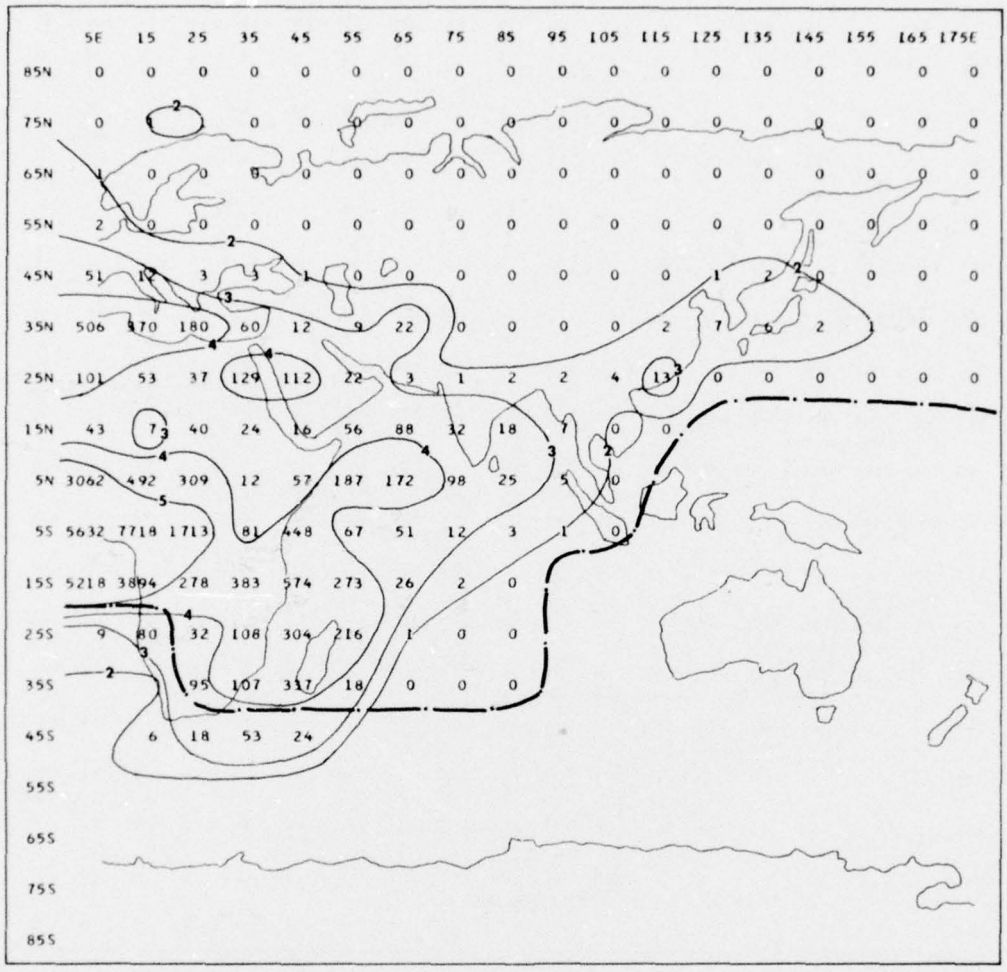

Figure 24. Distribution of the Estimated Number of Lightning Discharges for December 1972. The dash-dot line is the average threshold-sector line for the period August to December 1972. Values are in hundreds of discharges for 10-deg data blocks centered at the points shown. Isolines are number of discharges in powers of 10

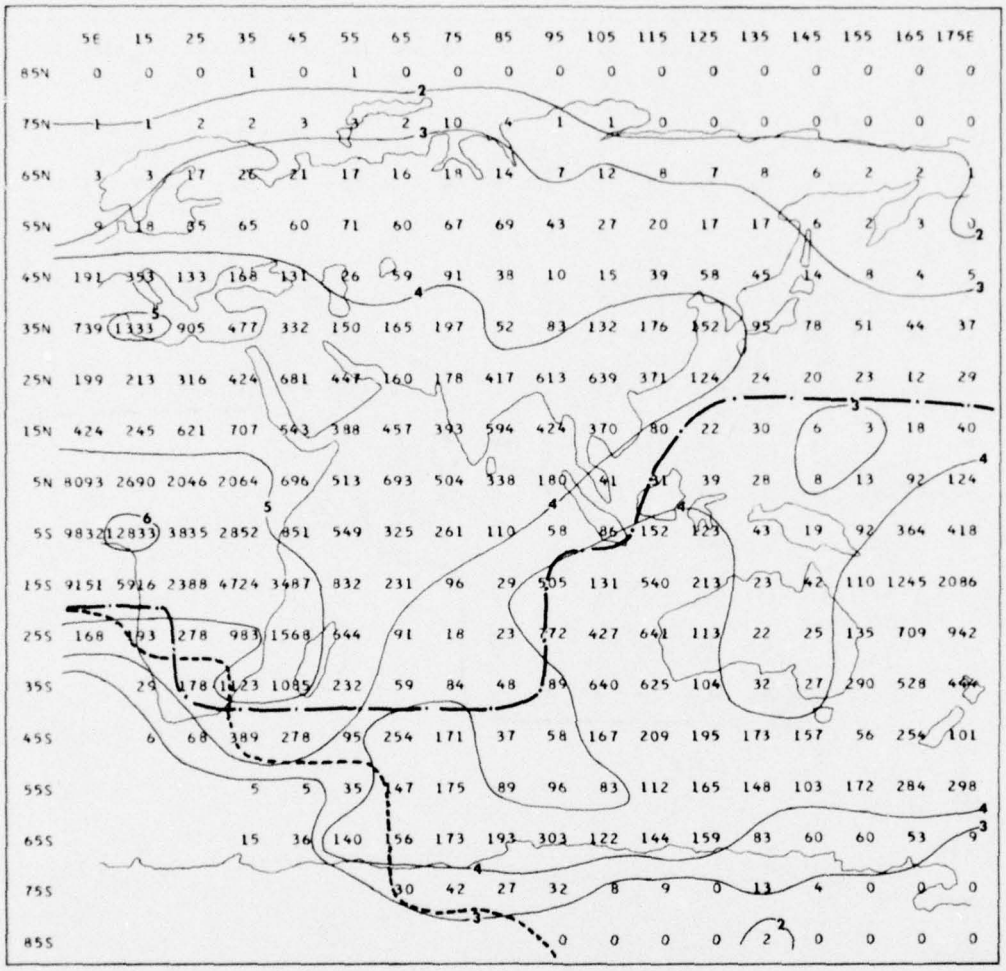

Figure 25. Distribution of the Estimated Number of Lightning Discharges for 1972. The broken line is the average threshold-sector line for the period January to July 1972 and the dash-dot line is that for the period August to December 1972. Values are in hundreds of discharges for 10-deg data blocks centered at the points shown. Isolines are number of discharges in powers of 10

have led to an overestimation of the number of lightning discharges if the received sferics did not follow the log-normal distribution in the extreme tails of the distribution.

Even a cursory examination of the threshold-sector line and the associated "spillover" for each month in Figures 13 through 25 indicates that the threshold-sector estimate was quite good, indeed, at least in terms of its effect on data coverage, for each month except August (Figure 20), September (Figure 21), and October (Figure 22). In these months there was considerable spillover of data and results south of the threshold-sector line and east of 95E longitude. It seems likely that the actual threshold-sector lines of the system for these months were simply departures from the mean estimate, even though it is impossible to state this with any assurance.

It should be pointed out that the combination of the round-off convention used in the estimate of the number of lightning discharges (that is, to the nearest 100 discharges), together with the constraint used in the Northern Hemisphere for the thunderstorm-day estimates (that is, at least 3 VLF signals in order to be counted), resulted in two monthly charts with estimated thunderstorm days but no estimated lightning discharges at one or two grid points. This occurred in January at 35N, 105E and in April at 65N, 35E and at 45N, 45E.

The thunderstorm-day charts (Figures 6 through 10) are not necessarily isomorphic to the respective lightning discharge charts (Figures 13, 16, 19, and 22) in every respect. The thunderstorm day is the report of the occurrence of at least one thunderstorm during a calendar day regardless of the number of storms that actually occurred. Therefore, if many storms occurred on a few days of the month, the respective distributions of thunderstorm days and lightning discharges could be quite different.

The validity of the estimates of the number of lightning discharges given in Figures 13 through 25 is not known, although the values of the incidence of discharge (to be given later in Section 3) which are based on the estimates of the number of lightning discharges, appear reasonable. It would be surprising if it were demonstrated that the distribution of the number of lightning discharges had no relationship to the state-of-nature even though the magnitude of the values may be doubtful; that is, at the very least, it seems likely that the results presented in Figures 13 through 25 represent an "electrical index" associated with the lightning discharge if, in fact, they do not represent the distribution of lightning discharges over the Eastern Hemisphere for 1972.

Heretofore, the lightning discharge distribution has been assumed to follow that of thunderstorm days.[3] A comparison of the estimates of these distributions produced herein for January, April, July, and October is as follows:

(1) January. The correspondence is close between the isoline pattern for January of thunderstorm days shown in Figure 4 and that of lightning discharges shown in Figure 13. A broad pattern, centered over Madagascar in Figure 4 and South Africa in Figure 13, extends into the Indian Ocean in both charts. Additionally, the "low center" at 15N, 15E in Figure 4 is present in Figure 13. Other reasonably close correspondences are the centers in both charts in the Mediterranean Sea, Arabia, India, Japan, and Southeast Asia. The patterns in Australia and the surrounding oceanic areas differ. (Again, one should view with caution the values at and south of 45S in all charts of the lightning discharge distribution.)

(2) April. The isoline pattern for April of thunderstorm days shown in Figure 6 and that for the number of lightning discharges shown in Figure 16 are dissimilar. The estimate of ten thunderstorm days centered at 35S, 45E in Figure 6 is associated with an estimated 185, 000 lightning discharges in Figure 16 in the same block (1, 011, 540 km^2), whereas the estimate of 29 thunderstorm days at 25N, 95E in Figure 6 is associated with an estimated 124, 000 lightning discharges (1, 119, 165 km^2) in Figure 16. As explained earlier, this type of reverse correspondence caused the isoline patterns to differ. The maximum centers of 30 thunderstorm days in Figure 6 at 15N, 45E and 25N, 105E have somewhat associated, closed, isolines of lightning discharge in Figure 16 of the order of 10^4, but the maximum center of thunderstorm days at 5N, 85E in Figure 6 does not correspond to a closed pattern of lightning discharge in Figure 16.

(3) July. The comparison for July produced mixed results. Although both the thunderstorm-day results shown in Figure 8 and the lightning discharge results shown in Figure 19 have centers of activity over Eurasia, the correspondence of specific centers is not very close. The thunderstorm-day center of 15 in Figure 8 at 15S, 115E is reflected as a lightning discharge center in Figure 19 of the order of 10^3 to the northeast of Australia. There is a very close correspondence in the thunderstorm day isoline of one in Figure 8 and the respective lightning discharge isoline of 10^2 shown in Figure 19, both of which span the northern extremity of the Eurasian continent.

(4) October. There is a reasonably close correspondence in the isoline patterns of estimated thunderstorm days shown in Figure 10 and that of lightning discharges shown in Figure 22. Both patterns have high centers of activity over much of Africa, the Mediterranean Sea, and India. If one tracks the extensive isoline of one in the thunderstorm-day chart shown in Figure 10 and compares it to the isoline of 10^2 in the lightning discharge chart shown in Figure 22, it becomes clear that the respective isoline patterns are similar.

Other observations concerning the estimated, monthly distributions of lightning discharge are:

(1) The center of the estimated number of lightning discharges in South and Central Africa is either the dominant center (for example, in January, February, September, October, November, and December shown, respectively, in Figures 13, 14, and 21 through 24) or is at least as large as that elsewhere for each month.

(2) In all the months that the combination of the minimum limits of threshold intensity and azimuthal sectoring permits a judgment (January through July in Figures 13 through 19), there always was present a center of lightning discharge to the east of Australia in the general vicinity of the Fiji Islands. There also is present always either a center or relatively high values in extreme western Australia and the coastal waters to the west.

(3) The distribution of lightning discharge in Southeast Asia is not as sharply defined in terms of closed isolines, nor is it as intense in order of magnitude as that in South and Central Africa. However, there always is present a value of at least 10^3 lightning discharges in Southeast Asia.

(4) There is either a center of lightning discharge or an isoline of at least 10^3 discharges in the Mediterranean Sea for each month.

(5) Surprisingly, there is a center of lightning discharge or an isoline of at least 10^3 discharges in Arabia for each month except July. The center in July, shown in Figure 19, is only of the order of 10^2 discharges.

(6) One may follow the effect of the march of the seasons in the Northern Hemisphere (0-179E) by looking at the general latitudinal position of the isoline of 10^2 lightning discharges that spans Eurasia in each month, as shown in Figures 13 through 24. In general terms, there is a march poleward of the 10^2 isoline from December to July. In July, as shown in Figure 19, there are two values in the Arctic at 85N latitude. The isoline of 10^2 discharges gradually recedes equatorward from July to the end of fall in December.

The estimated number of lightning discharges for 1972 is shown in Figure 25. The broken line is the threshold-sector line for the period January to July and the dash-dot line is the threshold-sector line for the period August to December. Therefore, one should realize that only the values north of the dash-dot line were based on data for all of 1972. It is to be recalled that values south of 45S were questionable since they were based on only a relatively few, intense, recorded signals and the assumption that the log-normal probability distribution was valid throughout the range of possible field strengths, including the extreme tails of the distribution. It seems unlikely that the 10^4 isoline of lightning discharge in the Southern Ocean and over Antarctica is valid.

The focus of thunderstorm days in Africa also is reflected in the distribution of lightning discharges shown in Figure 25. The highest estimate of 1,283,300 discharges over some 1,230,163 km^2 for all of 1972 is located at 5S, 15E in the focus of South Africa. There is a center of lightning discharge of the order of 10^5

discharges for the year over the Mediterranean Sea. The focus of thunderstorm days in Southeast Asia was weaker than that of Africa both in this study and in the WMO compilation. The estimated number of lightning discharges in Southeast Asia likewise was weaker than the African estimate by an order of magnitude in general (that is, 10^4 vs 10^5) and by two orders of magnitude for the respective central values (1, 283, 300 at 5S, 15E vs 42, 400 at 15N, 95E). There were relatively large estimates for the number of lightning discharges (of the order of 10^4) in Western Australia and over the islands in the South Pacific to the northeast of Australia.

If one accepts only values north of 45S latitude, as suggested earlier, it is interesting to compare the areal extent mapped out by the isoline of 10^4 discharges in Figure 25 with the region in the Eastern Hemisphere which is influenced by the monsoons. As mentioned earlier, Ramage[36] delineates the monsoon region as that enclosed between 35N and 25S and between 30W and 170E. The isoline of 10^4 discharges north of 45S in Figure 25 and the monsoon region after Ramage for the Eastern Hemisphere are reproduced in Figure 26. As we can see from Figures 25 and 26, the isolines of the highest three orders of magnitude (10^4, 10^5, and 10^6) of the estimated number of lightning discharges were enclosed within the monsoon region to a significant degree. This was not surprising since the tropics are considered the dominant source of thunderstorms on Earth.[3]

3.4 The Incidence of Lightning Discharge

A few investigators have given point or areal estimates of the incidence of lightning discharge. These estimates are presented in Table 9. As used here, the incidence of lightning discharge is defined as the occurrence of lightning discharges during a stormy period per unit area per unit time. The data of this study were amenable to an analysis of the distribution of the incidence of discharge for much of the Eastern Hemisphere.

As in most studies in meteorology, certain assumptions must be made. Following Horner,[11] the average extent of a "thunderstorm area" was assumed to be 1000 km^2; that is, during periods when thunderstorms were active in a data block, the average areal extent of the storm (or storms) was assumed to be 1000 km^2. The duration of thunderstorms on the average was assumed to be 3 hr in the tropics[10] and 1 hr in temperate and polar latitudes.[3] The "tropics" was somewhat arbitrarily defined as encompassing the area between 20N and 20S.

The incidence of lightning discharge at each grid point was estimated for the classic, climatologic months of January and April. First, an estimate of the number of discharges per thunderstorm day for the month was obtained. Each grid point in the distribution of the estimated number of lightning discharges for

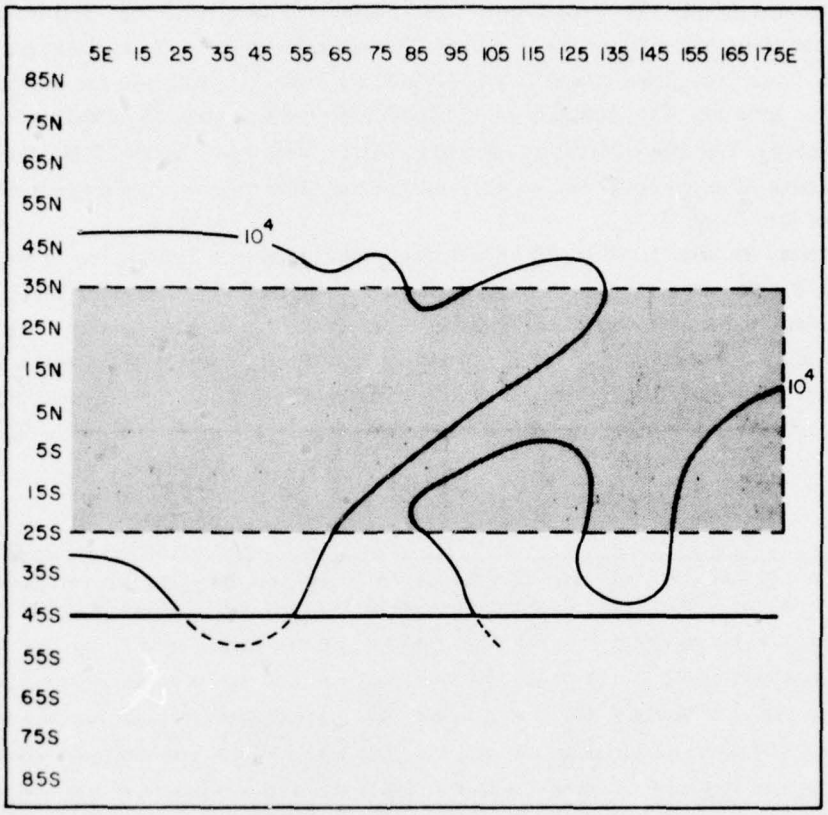

Figure 26. A Comparison of the Area Enclosed within the Isolines of 10^4 Lightning Discharges in the Eastern Hemisphere for 1972 North of 45S Latitude (heavy solid line) and the Region that is Usually under the Influence of the Monsoons (shaded box)

Table 9. Estimates of the Incidence of Lightning Discharge from the Literature (Units of km^{-2} sec^{-1})

Areas	Incidence of Lightning Discharge (km^{-2} sec^{-1})	Source
India	9×10^{-5}	Aiya (1968)
Main thunderstorm areas*	10^{-5}	Horner (1965)
World (range)	6×10^{-6} to 16×10^{-6}	Horner (1965)
World	10^{-4}	Brooks (1925)

*The main thunderstorm areas are the Americas, Africa, and Southeast Asia.

January and April, shown in Figures 13 and 16, respectively, was divided by the corresponding estimate of the number of thunderstorm days shown in Figures 4 and 6. This "resultant matrix" was divided by either 10, 800, 000 for the tropics (that is, 1000 km × 10, 800 sec) or 3, 600, 000 elsewhere (that is, 1000 km × 3, 600 sec). The final result at each grid point, shown in Figure 27 for January and Figure 28 for April, was an estimate of the incidence of lightning discharge in units of km^{-2} sec^{-1}.

Again, values at and south of 45S were questionable. The values in Figures 27 and 28 are negative, ordinary logarithms of the incidence of lightning discharge. Of course, the mantissa for each value is one less than the appropriate negative power of 10. For example, in Figure 27 at 15N, 125E, one finds the value 4.81 and may immediately surmise that the estimate of incidence for this data block is of the order of 10^{-5} lightning discharges km^{-2} sec^{-1} during a stormy period.

	5E	15	25	35	45	55	65	75	85	95	105	115	125	135	145	155	165	175E
85N	0.0	0.0	0.0	0.0	0.0	0.0	0.0	0.0	0.0	0.0	0.0	0.0	0.0	0.0	0.0	0.0	0.0	0.0
75N	4.56	0.0	0.0	0.0	0.0	0.0	0.0	0.0	0.0	0.0	0.0	0.0	0.0	0.0	0.0	0.0	0.0	0.0
65N	4.86	4.56	0.0	0.0	0.0	0.0	0.0	0.0	0.0	0.0	0.0	0.0	0.0	0.0	0.0	0.0	0.0	0.0
55N	0.0	0.0	0.0	5.03	0.0	0.0	0.0	0.0	0.0	0.0	0.0	0.0	0.0	0.0	0.0	0.0	0.0	0.0
45N	4.36	3.81	4.72	5.16	5.26	4.56	0.0	0.0	0.0	0.0	0.0	0.0	4.86	5.16	5.10	5.03	5.26	4.86
35N	4.14	3.56	3.54	3.82	4.72	4.78	4.76	4.47	5.16	5.03	0.0	4.86	4.65	4.45	4.50	4.63	4.61	4.73
25N	3.69	3.95	4.24	4.33	3.60	3.70	4.16	4.29	4.10	3.87	4.22	4.50	4.06	4.43	4.38	4.56	4.26	3.95
15N	3.75	0.0	5.33	4.98	5.18	5.51	5.58	5.03	5.03	5.33	5.21	5.03	4.81	4.79	5.03	0.0	5.33	5.33
5N	4.89	4.48	5.26	4.67	5.03	5.12	4.31	4.97	4.98	5.16	5.03	5.03	4.56	5.03	5.33	5.33	4.73	5.33
5S	3.96	4.14	4.60	4.04	4.64	4.57	4.92	4.89	5.26	5.40	5.33	4.73	4.86	5.16	5.03	4.19	4.01	4.12
15S	0.0	0.0	3.67	3.12	3.36	4.35	4.61	4.99	5.38	3.92	4.73	4.43	4.49	5.03	4.29	4.45	3.68	3.86
25S		0.0	2.92	3.12	3.23	3.77	4.40	5.16	4.56	2.56	3.62	3.32	4.08	4.26	4.26	3.86	3.78	3.78
35S			3.65	3.05	3.39	4.12	4.86	3.51	4.26	4.19	2.74	3.12	3.65	4.26	4.56	3.86	0.0	3.12
45S				3.16	2.66	3.19	3.04	3.54	4.46	4.08	4.02	3.71	3.54	0.0	3.82	0.0	0.0	3.63
55S					3.86	3.56	3.15	3.43	4.03	4.01	3.84	3.68	3.23	3.56	3.95	4.08	3.50	3.90
65S				3.86	3.54	3.06	3.27	3.21	3.20	3.14	3.57	3.45	3.54	3.48	3.71	3.95	3.78	0.0
75S							3.30	3.30	3.51	3.60	0.0	4.08	0.0	0.0	4.08	0.0	0.0	0.0
85S										0.0	0.0	0.0	0.0	4.26	0.0	0.0	0.0	0.0

Figure 27. Distribution of the Incidence of Lightning Discharge (km^{-2} sec^{-1}) for January 1972. The dash-dot line is the threshold-sector line for the period January to July 1972. Values are negative, ordinary logarithms for 10-deg data blocks centered at the points shown.

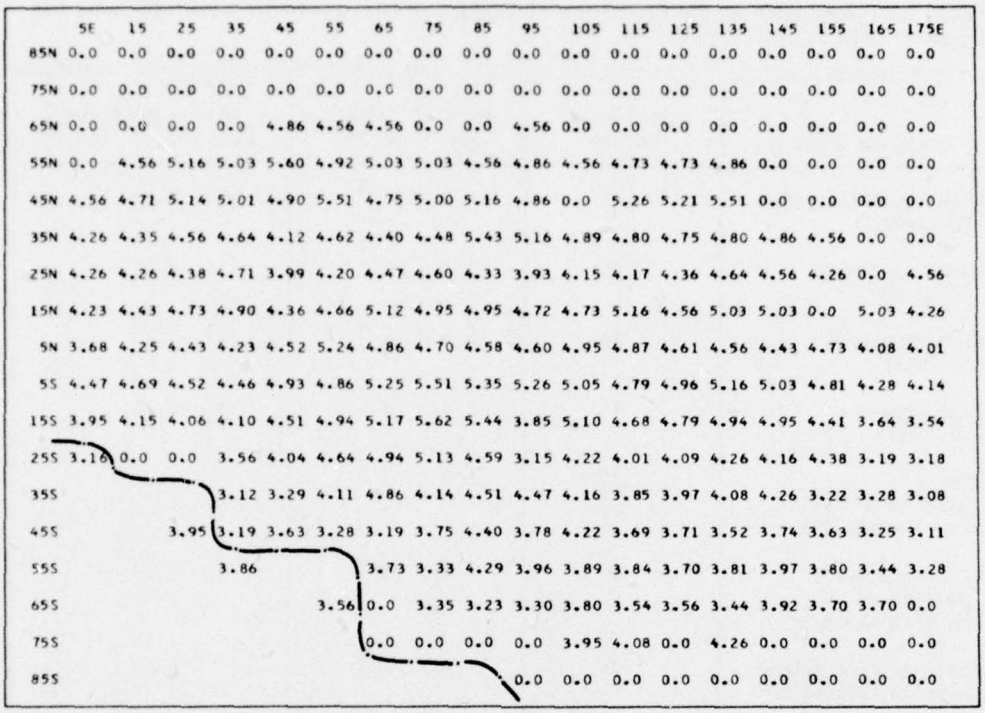

	5E	15	25	35	45	55	65	75	85	95	105	115	125	135	145	155	165	175E
85N	0.0	0.0	0.0	0.0	0.0	0.0	0.0	0.0	0.0	0.0	0.0	0.0	0.0	0.0	0.0	0.0	0.0	0.0
75N	0.0	0.0	0.0	0.0	0.0	0.0	0.0	0.0	0.0	0.0	0.0	0.0	0.0	0.0	0.0	0.0	0.0	0.0
65N	0.0	0.0	0.0	0.0	4.86	4.56	4.56	0.0	0.0	4.56	0.0	0.0	0.0	0.0	0.0	0.0	0.0	0.0
55N	0.0	4.56	5.16	5.03	5.60	4.92	5.03	5.03	4.56	4.86	4.56	4.73	4.73	4.86	0.0	0.0	0.0	0.0
45N	4.56	4.71	5.14	5.01	4.90	5.51	4.75	5.00	5.16	4.86	0.0	5.26	5.21	5.51	0.0	0.0	0.0	0.0
35N	4.26	4.35	4.56	4.64	4.12	4.62	4.40	4.48	5.43	5.16	4.89	4.80	4.75	4.80	4.86	4.56	0.0	0.0
25N	4.26	4.26	4.38	4.71	3.99	4.20	4.47	4.60	4.33	3.93	4.15	4.17	4.36	4.64	4.56	4.26	0.0	4.56
15N	4.23	4.43	4.73	4.90	4.36	4.66	5.12	4.95	4.95	4.72	4.73	5.16	4.56	5.03	5.03	0.0	5.03	4.26
5N	3.68	4.25	4.43	4.23	4.52	5.24	4.86	4.70	4.58	4.60	4.95	4.87	4.61	4.56	4.43	4.73	4.08	4.01
5S	4.47	4.69	4.52	4.46	4.93	4.86	5.25	5.51	5.35	5.26	5.05	4.79	4.96	5.16	5.03	4.81	4.28	4.14
15S	3.95	4.15	4.06	4.10	4.51	4.94	5.17	5.62	5.44	3.85	5.10	4.68	4.79	4.94	4.95	4.41	3.64	3.54
25S	3.16	0.0	0.0	3.56	4.04	4.64	4.94	5.13	4.59	3.15	4.22	4.01	4.09	4.26	4.16	4.38	3.19	3.18
35S				3.12	3.29	4.11	4.86	4.14	4.51	4.47	4.16	3.85	3.97	4.08	4.26	3.22	3.28	3.08
45S			3.95	3.19	3.63	3.28	3.19	3.75	4.40	3.78	4.22	3.69	3.71	3.52	3.74	3.63	3.25	3.11
55S				3.86			3.73	3.33	4.29	3.96	3.89	3.84	3.70	3.81	3.97	3.80	3.44	3.28
65S						3.56	0.0	3.35	3.23	3.30	3.80	3.54	3.56	3.44	3.92	3.70	3.70	0.0
75S							0.0	0.0	0.0	0.0	3.95	4.08	0.0	4.26	0.0	0.0	0.0	0.0
85S										0.0	0.0	0.0	0.0	0.0	0.0	0.0	0.0	0.0

Figure 28. Distribution of the Incidence of Lightning Discharge (km^{-2} sec^{-1}) for April 1972. The dash-dot line is the threshold-sector line for the period January to July 1972. Values are negative, ordinary logarithms for 10-deg data blocks centered at the points shown

Estimates of the incidence of lightning discharge by latitude zones are given in Table 10 for January 1972 and Table 11 for April 1972. The respective estimates for the two months agree consistently in order of magnitude, although they vary from a close agreement of 96 percent (that is, 2.3×10^{-5} km^{-2} sec^{-1} compared to 2.4×10^{-5} km^{-2} sec^{-1}) for the estimates in the zone of high north latitudes to a disagreement by a factor of 3 for the estimate of all available data for each month (that is, 3.6×10^{-4} compared to 1.1×10^{-4} km^{-2} sec^{-1}).

Aiya[10] estimated that, in general, the incidence of lightning discharge in India is 9×10^{-5} km^{-2} sec^{-1} as indicated in Table 9. The estimates on the average of this study for those data blocks that include some portion of India were 3.5×10^{-5} km^{-2} sec^{-1} for both January and April of 1972. The estimates of this study for that portion of the tropics in the Northern and Eastern Hemisphere, (that is, between the equator and 20N and between the Greenwich Meridian and 179E) were 1.6×10^{-5} km^{-2} sec^{-1} for January 1972 and 3.4×10^{-5} km^{-2} sec^{-1} for April 1972, as shown in Tables 10 and 11, respectively.

Table 10. Estimate of the Incidence of Lightning Discharge by Latitude Zone for January 1972 (Units of km^{-2} sec^{-1})

Latitude Zone	Number of Values	Sum of Values (km^{-2} sec^{-1})	Average Value (10^{-5} km^{-2} sec^{-1})
High north latitudes (60N-90N)	3	6.9×10^{-5}	2.3
Middle latitudes (21N-59N)	48	3.0×10^{-3}	6.3
N. H. tropics (0-20N)	34	5.5×10^{-4}	1.6
S. H. tropics (0-20S)	34	2.8×10^{-3}	8.3
Other (part of 21S-91S, see Figure 27)	72	2.8×10^{-2}	38
N. Hemisphere portion of E. Hemisphere	85	3.4×10^{-3}	4.2
Eastern Hemisphere tropics (20N-20S)	68	3.4×10^{-3}	5.0
All grid point estimates*	191	3.4×10^{-2}	36

*Includes values along and south of 45S latitude, which may be questionable.

Horner[11] gave an order of magnitude estimate of the incidence of discharge of 10^{-5} km^{-2} sec^{-1} for the "main thunderstorm areas of the world" as shown in Table 9. A roughly comparable estimate is that of this study for the incidence of discharge in the tropics of the eastern Hemisphere (that is, 20N to 20S) as given in Table 10 for January 1972 and Table 11 for April 1972. These estimates were 5.0×10^{-5} km^{-2} sec^{-1} for January and 2.6×10^{-5} km^{-2} sec^{-1} for April.

Horner[11] also gave a range of estimates, based on various techniques mentioned in Section i, for the global incidence of lightning discharge. These estimates ranged from 6×10^{-6} km^{-2} sec^{-1} to 16×10^{-6} km^{-2} sec^{-1} as shown in Table 9. One may infer from Brook's work,[8] as mentioned in Section 1 and presented in Table 9, that the global incidence of lightning discharge is of the order of 10^{-4} km^{-2} sec^{-1}. The most reliable planetary-scale estimates of this study of the incidence of discharge were for the Northern Hemisphere (0-179E). The estimate of the incidence for January 1972 for this area was 4.2×10^{-5} km^{-2} sec^{-1} as given

Table 11. Estimate of the Incidence of Lightning Discharge by Latitude Zone for April 1972 (Units of km^{-2} sec^{-1})

Latitude Zone	Number of Values	Sum of Values (km^{-2} sec^{-1})	Average Value (10^{-5} km^{-2} sec^{-1})
High north latitudes (60N-90N)	4	9.6×10^{-5}	2.4
Middle latitudes (21N-59N)	59	1.7×10^{-3}	2.8
N. H. tropics (0-20N)	35	1.2×10^{-3}	3.4
S. H. tropics (0-20S)	36	1.5×10^{-3}	4.2
Other (part of 21S-91S, see Figure 28)	70	1.8×10^{-2}	2.5
N. Hemisphere portion of E. Hemisphere	98	2.9×10^{-3}	3.0
Eastern Hemisphere tropics (20N-20S)	106	2.7×10^{-3}	2.6
All grid point estimates*	204	2.2×10^{-2}	1.1

*Includes values along and south of 45S latitude, which may be questionable.

in Table 10 and 3.0×10^{-5} km^{-2} sec^{-1} for April 1972 as given in Table 11. The estimate of the average incidence of discharge for all grid points that were available above the threshold-sector line in January 1972 was 3.6×10^{-4} km^{-2} sec^{-1} and the commensurate estimate for April 1972 was 1.1×10^{-4} km^{-2} sec^{-1} as indicated in Tables 10 and 11, respectively. However, values in high latitudes of the Southern Hemisphere that were used in these estimates were questionable.

3.5 Areal Concentration of Lightning Discharge

There seems to be no estimate available in the literature for the areal concentration of lightning discharge. This parameter of thunderstorm activity, as used here, is the number of lightning discharges per unit area over some time period irrespective of the specific areal extent of thunderstorm activity which caused the discharges. In other words, it is simply the number of discharges per gross area.

This parameter is not the same, therefore, as the "lightning discharge density," which is always related to the extent of area under the influence of thunderstorms.

An estimate of the distribution of the areal concentration of lightning discharge for 1972 was obtained by dividing the value at each grid point in the yearly estimate of the total number of lightning discharges (Figure 25) by the area of the 10-deg, latitude-longitude block that encloses the grid point. The areas for the nine blocks from pole to equator in a hemisphere are listed in Table 12. These values were calculated by a straightforward application of spherical trigonometry on the basis of a spherical Earth (r = 6371 km).

Table 12. Areas on Earth Bounded by Any Two Meridians 10-deg Apart and the Two, Indicated Parallels; the Average Areal Concentration of Lightning Discharge in the Northern Hemisphere Within the Indicated Parallel Bounds

Area Number	Parallel Bounds (degrees)	Area (km^2)	Average Areal Concentration of Discharge (km^{-2})
1	0-10	1,230,163	1.31×10^{-1}
2	10-20	1,192,786	3.94×10^{-2}
3	20-30	1,119,165	3.48×10^{-2}
4	30-40	1,001,540	4.09×10^{-2}
5	40-50	873,180	1.27×10^{-3}
6	50-60	708,288	6.73×10^{-3}
7	60-70	521,875	2.68×10^{-3}
8	70-80	319,606	8.58×10^{-4}
9	80-90	107,625	9.33×10^{-4}

The yearly estimate of the distribution of the areal concentration of lightning discharge is given in Figure 29. All values are negative, ordinary logarithms of the areal concentration of discharge except the value of 0.02 at 5S, 15E which is positive (that is, the logarithm of 1,283,300 discharges at 5S, 15E from Figure 25 divided by 1,230,163 km^2 from Table 12.) The threshold-sector line and the concomitant explanation are the same for the areal concentration of discharge as that for the yearly estimate for 1972 of the number of lightning discharges given in Figure 25 and on page 59. Recall that only the values in Figure 25 north of the dash-dot line are based on data for all of 1972.

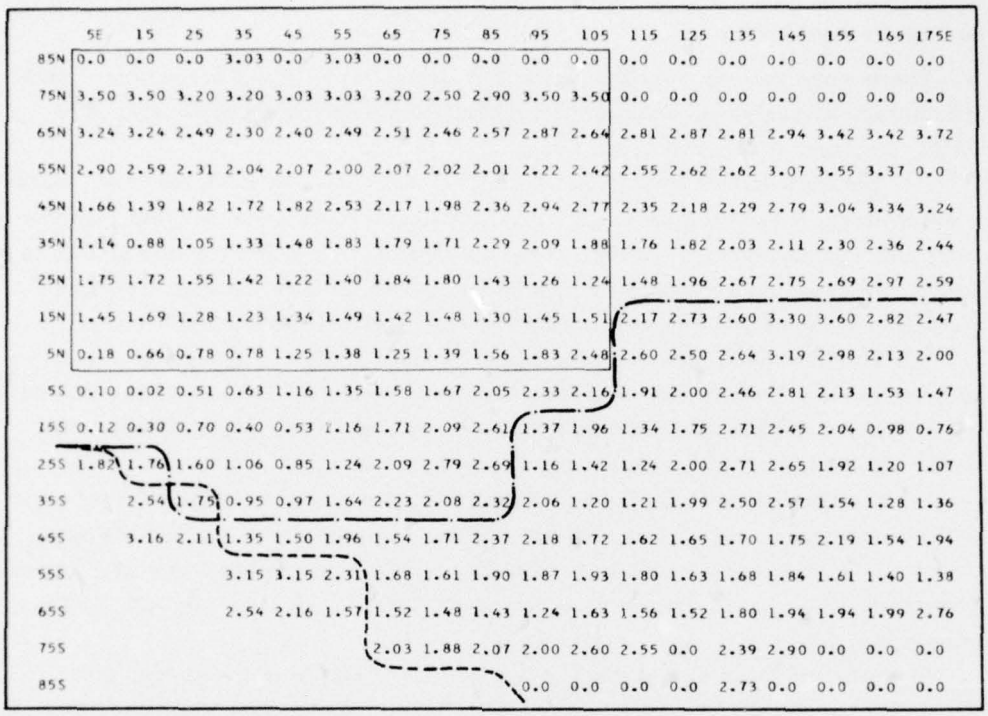

	5E	15	25	35	45	55	65	75	85	95	105	115	125	135	145	155	165	175E
85N	0.0	0.0	0.0	3.03	0.0	3.03	0.0	0.0	0.0	0.0	0.0	0.0	0.0	0.0	0.0	0.0	0.0	0.0
75N	3.50	3.50	3.20	3.20	3.03	3.03	3.20	2.50	2.90	3.50	3.50	0.0	0.0	0.0	0.0	0.0	0.0	0.0
65N	3.24	3.24	2.49	2.30	2.40	2.49	2.51	2.46	2.57	2.87	2.64	2.81	2.87	2.81	2.94	3.42	3.42	3.72
55N	2.90	2.59	2.31	2.04	2.07	2.00	2.07	2.02	2.01	2.22	2.42	2.55	2.62	2.62	3.07	3.55	3.37	0.0
45N	1.66	1.39	1.82	1.72	1.82	2.53	2.17	1.98	2.36	2.94	2.77	2.35	2.18	2.29	2.79	3.04	3.34	3.24
35N	1.14	0.88	1.05	1.33	1.48	1.83	1.79	1.71	2.29	2.09	1.88	1.76	1.82	2.03	2.11	2.30	2.36	2.44
25N	1.75	1.72	1.55	1.42	1.22	1.40	1.84	1.80	1.43	1.26	1.24	1.48	1.96	2.67	2.75	2.69	2.97	2.59
15N	1.45	1.69	1.28	1.23	1.34	1.49	1.42	1.48	1.30	1.45	1.51	2.17	2.73	2.60	3.30	3.60	2.82	2.47
5N	0.18	0.66	0.78	0.78	1.25	1.38	1.25	1.39	1.56	1.83	2.48	2.60	2.50	2.64	3.19	2.98	2.13	2.00
5S	0.10	0.02	0.51	0.63	1.16	1.35	1.58	1.67	2.05	2.33	2.16	1.91	2.00	2.46	2.81	2.13	1.53	1.47
15S	0.12	0.30	0.70	0.40	0.53	1.16	1.71	2.09	2.61	1.37	1.96	1.34	1.75	2.71	2.45	2.04	0.98	0.76
25S	1.82	1.76	1.60	1.06	0.85	1.24	2.09	2.79	2.69	1.16	1.42	1.24	2.00	2.71	2.65	1.92	1.20	1.07
35S		2.54	1.75	0.95	0.97	1.64	2.23	2.08	2.32	2.06	1.20	1.21	1.99	2.50	2.57	1.54	1.28	1.36
45S		3.16	2.11	1.35	1.50	1.96	1.54	1.71	2.37	2.18	1.72	1.62	1.65	1.70	1.75	2.19	1.54	1.94
55S				3.15	3.15	2.31	1.68	1.61	1.90	1.87	1.93	1.80	1.63	1.68	1.84	1.61	1.40	1.38
65S				2.54	2.16	1.57	1.52	1.48	1.43	1.24	1.63	1.56	1.52	1.80	1.94	1.94	1.99	2.76
75S							2.03	1.88	2.07	2.00	2.60	2.55	0.0	2.39	2.90	0.0	0.0	0.0
85S										0.0	0.0	0.0	0.0	2.73	0.0	0.0	0.0	0.0

Figure 29. Distribution of the Areal Concentration of Lightning Discharge (km^{-2}) for 1972. The broken line is the average threshold-sector line for the period January to July 1972 and the dash-dot line that for the period August to December 1972. Values are negative, ordinary logarithms (except for that at 5S, 15E which is positive) for 10-deg data blocks centered at the points shown. Solid box is the area of maximum data coverage in the Northern Hemisphere

One may approximate the latitudinal change of the areal concentration of lightning discharge from a study of the area of maximum data coverage in the Northern Hemisphere (Figure 29), as outlined by the solid box (that is, by the grid points of 5N to 85N latitude and 5E to 105E longitude). The average areal concentration of discharge for the 10-deg zones of latitude with central points as shown in Figure 29 (that is, 5N, 15N, 25N, and so on) is presented in Table 12. The general trend evident from Table 12 and Figure 29 was that the average, areal concentration of lightning discharge decreased with geographic latitude in 1972 in the Northern Hemisphere quadrant of the Eastern Hemisphere. The areal concentration of discharge was three orders of magnitude higher on the average in the equatorial zone (0-10N) than in the polar zone (80N-90N) for 1972.

3.6 Possible Sources of Error

There were various possible sources of error in the initial collection of data and subsequent analyses, some of which have been mentioned previously. The known, possible sources of error were:

(1) The instrument error is not known in quantitative terms. However, errors in calibration, the setting of the gating circuits, and so on, are possible. Moreover, two signals that are incident at the antenna at precisely the same instant in time would cause an erroneous, distorted waveform to be recorded. The time resolution of the signal monitor for individual, received sferics is 10^{-5} sec.

(2) The threshold arrays (lower limits on the probability integrals) are only mean estimates, dependent to a large extent on propagation laws at VLF. Pierce[32] stated that propagation at VLF is subject to geographic, geomagnetic, and temporal variability, none of which is known with certainty.

(3) The important statistics listed in Table 2, which generally are point estimates in the mean, may not be suitable for this work. Since there is wide agreement that the standard deviation of received sferics ranges from 6 to 8 dB, we may appreciate the effect on the analyses of varying this sample statistic, other things being equal.

An estimate of the distribution of the number of lightning discharges for August 1972 with standard deviations of 6, 7, and 8 dB are shown in Figure 30. The middle distribution in Figure 30, presented in hundreds of discharges with a standard deviation of 7 dB, is the same as that given previously in Figure 20 for August 1972. For a given threshold value at a grid point [that is, a given lower limit on the probability integrals as shown in Eq. (13)], the estimate of the number of lightning discharges increases with increasing standard deviation as shown in Figure 30 (or remains the same due to round-off to the nearest 100 discharges). Since standard deviation is a measure of dispersion, the probability of occurrence above a given threshold value (namely, percentile) increases with increasing standard deviation. But the probability integrals that are thus effected enter into Eq. (13) in the denominator with the result that the estimate of the number of lightning discharges decreases at a grid point with an increase in standard deviation.

A detailed analysis of error of the values in Figure 30 is not warranted because of the uncertainties associated with the other sample statistics given in Table 2 that affect the distribution of sferics. In general, there is little or no change in the estimates of the number of lightning discharges (to the nearest 100 discharges) in high north and south latitudes where the threshold array places the

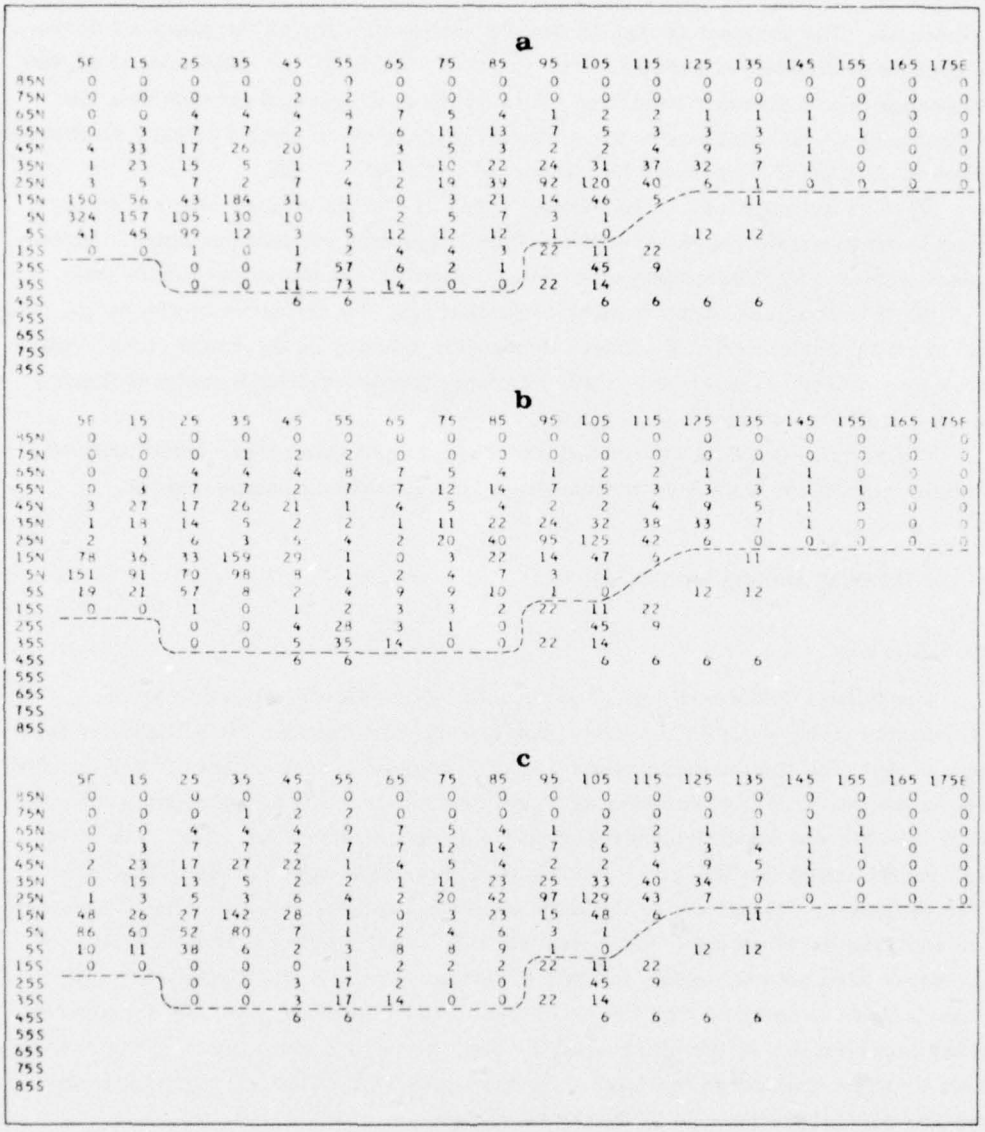

Figure 30. Comparison of the Distributions of Lightning Discharge for August 1972 for Standard Deviations of Received Sferics of (a) 6 dB, (b) 7 dB, and (c) 8 dB. Values are in hundreds of discharges for 10-deg data blocks centered at the points shown. The broken line is the average threshold-sector line for the period August to December 1972

appropriate t value* in the extreme "left" and "right" tails of the respective distributions. The greatest change in results caused by varying the standard deviation alone is roughly 50 percent. For example, at 5N, 5E the estimates of 32,400 discharges for a standard deviation (SD) of 6 dB is 47 percent greater than the estimate of 15,100 discharges for a SD of 7 dB; and the estimate of 8600 discharges for a SD of 8 dB is 57 percent less than that for a SD of 7 dB.

(4) The distributions of the various types of sferics studied may not be log-normal over certain ranges of values of the respective random variables. Indeed, these sferics may follow some other distribution for extensive periods of time.

(5) The analyses of the number of discharges, the incidence of discharge, and the areal concentration of discharge depend for efficacy on the rough, empirical equations quoted or developed in this section. Moreover, these analyses depend on assumptions that may not be valid.

The various possible sources of error mentioned above were very likely of a random nature and may have compensated for each other to some degree.

4. CONCLUSIONS AND RECOMMENDATIONS

4.1 Conclusions

The following distributions of parameters were developed in this study: (1) thunderstorm days for January, April, July, and October of 1972 and for the entire year; (2) the number of lightning discharges for each month of 1972 and for the entire year; (3) the incidence of lightning discharge for January and April of 1972; and (4) the areal concentration of lightning discharge for 1972. The study was restricted to the Eastern Hemisphere and the data were unique in that no sferics data on a planetary-scale basis have been heretofore available. Therefore, the analyses based on these data resulted in first estimates of the distribution of the above parameters, except for that of thunderstorm days. There were few uncertainties associated with the estimates of thunderstorm days, but there were many uncertainties in the other analyses and, therefore, the results of these analyses must be considered tentative. Nevertheless, the following conclusions for the Eastern Hemisphere in 1972 may be stated:

(1) The thunderstorm-day charts of this study differ considerably from the mean, monthly charts of the WMO that were based on data compiled in 1953. One possible cause of the differences was that the monthly charts of this study, that

*Where $t = (T_o - \overline{T})/\sigma$; T_o and $\overline{T}$ are the threshold intensity in field strength at a grid point and the mean field strength of the distribution, respectively; σ is standard deviation.

were based on one year of data, could represent an anomaly from the mean pattern of the WMO charts. Another cause of difference that seems incontrovertible was that in the WMO compilation of the data there were extensive areas on Earth with a void of data coverage. These areas include the oceans, North Africa, Arabia, the Mediterranean Sea, and Southeast China. It has been shown in this study that there were many more thunderstorm days in these areas in 1972 than reported by the WMO in the mean.

(2) A first estimate of the distribution of the number of lightning discharges over a large area of Earth was presented in Figures 13 through 25. The validity of the magnitude of any one estimate at a grid point or, indeed, of all the estimates, is not known. However, the magnitude of the values relative to each other and the isoline patterns probably represent a useful index of "electrical activity" over a broad area of Earth.

(3) There was a close correspondence between the isoline patterns of thunderstorm days and lightning discharges for the months of January and October. There was little correspondence, in general, between these isoline patterns for April and July. (Heretofore, the assumption has been made frequently that the distributions were the same.)

(4) Central and South Africa were the dominant foci of lightning occurrence on a yearly basis and either a relatively high center, or the highest center of activity on a monthly basis. The occurrence of lightning was relatively high in the Mediterranean Sea and Arabia for most months. The occurrence of lightning in Southeast Asia was consistently smaller in magnitude than in Africa. There was always present a relatively high occurrence of lightning in Eastern and Western Australia and in the adjacent oceanic areas.

(5) The latitudinal occurrence of lightning discharges was shown to follow Sun northward over Eurasia from January to a maximum poleward thrust in July with occurrences of discharge over the Arctic. The occurrence of discharge then receded equatorward from the Arctic from July to the end of fall in December.

(6) An estimate of the distribution of the incidence of lightning discharge for January and April was presented in Figures 27 and 28, respectively. A breakdown of the average incidence of discharge by zones of latitude was presented in Tables 10 and 11. The most reliable planetary-scale estimate of the average incidence of discharge was 4.2×10^{-5} km^{-2} sec^{-1} for January and 3.0×10^{-5} km^{-2} sec^{-1} for April over the Northern Hemisphere (0-179E). An average incidence of discharge of 3.6×10^{-4} km^{-2} sec^{-1} was obtained for January and 1.1×10^{-4} sec^{-1} for April over the Eastern Hemisphere as a whole, but these results were considered less reliable due to uncertainties in the analysis.

(7) An estimate of the distribution of the areal concentration of lightning discharge was presented in Figure 29. There was evidence, based on an analysis in

the Northern Hemisphere (0-105E), that, in general, the areal concentration of discharge decreased with geographic latitude.

4.2 Recommendations

(1) There is much current interest in the relationship between thunderstorm days and the incidence of lightning discharge.[32] A direct extension of this work would be the development of laws that relate these parameters on a monthly and yearly basis.

(2) Very useful information on the diurnal variation of thunderstorm activity could be developed from these data. This is especially true for oceanic areas where frequently the diurnal variation is assumed to be constant. Estimates of the diurnal variation of thunderstorm activity for Africa, Eurasia, Southeast Asia, Australia, and the Eastern Hemisphere as a whole could be developed.

(3) One could analyze the extensive data in 6-hr increments to obtain estimates of the number of active thunderstorms that occur on Earth at any one time. This information may be useful to those who study the general circulation of the atmosphere.

(4) An analysis of the data could be performed in 6-hr increments and estimates made of the disturbed-weather electrical field over a large area of Earth that is generated by thunderstorms.

(5) One could use both visible and infrared satellite photographs for 1972 that show discernible, large, isolated, cumulonimbus clouds and a 6-hr "electrical index" developed from these data to attempt to relate the sferics count to the vertical and areal extent of the cloud shield. A strong correlation could lead to a useful analysis of the electrical intensity of thunderstorms as it relates to the diameter-to-depth ratio of clouds.

(6) A challenging investigation would be to attempt to fit an empirical, statistical distribution to the occurrence of lightning discharge on a 6-hr basis over a large area of Earth. These data are amenable to such investigation.

(7) One could build evidence based on these data directed at showing that nature dominantly selects the ice process in cloud electrification over that of liquid water. The steps in this investigation would be first to develop a bench mark of electrical activity, E, over a grid. This could be done by normalizing the sferic counts by the use of the threshold arrays. Then one could regress E onto latitude and perhaps obtain a rough fit to the data. Next, one could find a best-fit approximation for E in terms of geographic latitude and the mean terrain height. It is hoped that, the fit would be better than previously. Finally, one could find the best-fit approximation of E in terms of latitude, ϕ, mean terrain height, H_t, and the freezing level, FL, of the form

$$E = f(\phi,\ H_t,\ FL) \quad . \tag{16}$$

If one could assert, with a high level of confidence, that this best-fit approximation was a statistically significant improvement over the previous ones, then attention could be directed to developing a physical explanation of why the improvement came about.

References

1. Chi-Chen, L., and Chi-Zhang, L. (1966) Problems on the geographical distribution of the atmospheric electric field induced by thunderstorm activities, AD 660 541, Contract No. AF(628)-5073, Emm 67-165 Translations, Translated from Acta Meteorologica Sinica 36:275-279.
2. Viemeister, P.E. (1961) The Lightning Book, Doubleday, New York, 316 pp.
3. Horner, F. (1964) Radio noise from thunderstorms, Advances in Radio Research, Vol. 2, Academic Press, New York, pp. 121-204.
4. Martin, J.N., and Hildebrand, V.W. (1965) Statistical evaluation of sferics distribution, NOLC Rept. 628, Project No. WR5-0062 AD620459, Naval Ordnance Laboratory, Corona, Calif, 95 pp.
5. Byers, H.R. (1965) The relation of lightning and thunderstorms to meteorological conditions, Problems of Atmospheric and Space Electricity, Elsevier Pub. Co., Amsterdam, pp. 491-496.
6. World Meteorological Organization (1953) Part 1, Publ. No. 21, TP 6.
7. World Meteorological Organization (1956) Part 2, Publ. No. 21, TP 6.
8. Brooks, C.E.P. (1925) The distribution of thunderstorms over the globe, Met. Office Geophys. Mem. and Profl. Notes, No. 24, London, 147-164.
9. Heydt, G., and Volland, H. (1964) A new method for location of thunderstorms and counting their lightning discharges from a single observing station, J. Atmos. Terr. Phys. 26:85-104.
10. Aiya, S.V.C. (1968) Lightning and power systems, Electro-Technology, J. Soc. Electronic Engineers, Bangalore 12(No. 1):1-12.
11. Horner, F. (1965) Radio noise in space originating in natural terrestrial sources, Planet. Space Sci. 13:1137-1150.
12. Huschke, R.E., Ed. (1959) Glossary of Meteorology, Am. Meteor. Soc., Boston, 638 pp.
13. Ishikawa, H. (1960) Nature of lightning discharges as origins of atmospherics, Proc. Res. Inst. Atmos., Nagoya University, 8A:1-274.

14. Pierce, E.T., Arnold, H.R., and Dennis, A.S. (1962) Very-low-frequency Atmospherics Due to Lightning Flashes, Final Rept. SRI Project No. 3738, Contract No. AF33(657)-7009, Stanford Research Institute, Menlo Park, Calif., 132 pp.

15. Chalmers, J.A. (1967) Atmospheric Electricity, 2nd ed., Pergamon Press, New York, 515 pp.

16. Pierce, E.T. (1955) Electrostatic field-changes due to lightning discharges, Quart. J. Roy. Meteor. Soc. 81:211-228.

17. MacKerras, D. (1968) A comparison of discharge processes in cloud and ground lightning flashes, J. Geophys. Res. 73:1175-1183.

18. Takeuti, T. (1965) Studies on thunderstorm electricity, Proc. Res. Inst. Atmos., Nagoya University, 12A:1-70.

19. Workman, E.G., Brook, M., and Kitagawa, N. (1960) Lightning and charge storage, J. Geophys. Res. 65:1513-1517.

20. Pierce, E.T. (1970) Latitudinal variation of lightning parameters, J. Appl. Meteor. 9:194-195.

21. Smith, L.G. (1957) Intracloud lightning discharges, Quart. J. Roy. Meteor. Soc. 83:103-111.

22. Ogawa, T., and Brook, M. (1964) Nature of lightning discharges as origins of atmospherics, J. Geophys. Res. 69:5141-5150.

23. Takagi, M. (1961) The mechanism of discharges in a thundercloud, Proc. Res. Inst. Atmos., Nagoya University, 8B:1-105.

24. Moyer, V.E. (1974) Personal communication.

25. Popov, A.S. (1896) Apparatus for reception and recording of electrical oscillations, J. Russ. Phys. Chem. Soc. 28:7-9.

26. Leushin, N.I. (1964) Explanation of the cause of non-correspondence of sferics centers and weather conditions, AD 653 173, Contract No. AF19(628)-3880, Am. Meteor. Soc. Translation, Translated from Trudy Glavnaia Geofizicheskaia Observatoriia, Leningrad 157:76-84.

27. Barkalova, K.N. (1964) Relation between the number of thunderstorms and the amount of sferics that produce a field strength greater than a given level, AD 653 172, Contract No. AF19(628)-3880, Am. Meteor. Soc. Translation, Translated from Trudy Glavnaia Geofizicheskaia Observatoriia, Leningrad, 157:85-86.

28. Horner, F. (1958) The relationship between atmospheric radio noise and lightning, J. Atmos. Terr. Phys. 13:140-154.

29. Malan, D.J. (1958) Radiation from lightning discharges and its relation to the discharge process, in Recent Advances in Atmospheric Electricity, Pergamon Press, New York, pp. 557-563.

30. Kitagawa, N., and Brook, M. (1960) A comparison of intracloud and cloud-to-ground lightning discharges, J. Geophys. Res. 65:1927-1931.

31. Horner, F., and Bradley, P.A. (1964) The spectra of atmospherics from near lightning discharges, J. Atmos. Terr. Phys. 26:1155-1166.

32. Pierce, E.T. (1973) Personal communication.

33. Horner, F. (1960) Narrow-band atmospherics from two local thunderstorms, J. Atmos. Terr. Phys. 21:13-25.

34. Bailey, T.W. (1972) Personal communication.

35. Kalakowsky, C.B., and Lewis, E.A. (1966) VLF sferics of very large virtual source strength, Physical Science Research Papers, No. 261, AFCRL Project No. 4603, Air Force Cambridge Research Laboratories, Bedford, Mass.

36. Ramage, C.S. (1971) Monsoon Meteorology, Academic Press, New York, 296 pp.

37. Griffiths, J.F. (1974) *Personal communication.*

38. Pierce, E.T. (1969) The thunderstorm as a source of atmospheric noise at frequencies between 1 and 100 kHz, Tech. Rept. 2, SRI Project No. 7045, Contract No. DASA01-68-C-0073, Stanford Research Institute, Menlo Park, Calif., 90 pp.

39. Pierce, E.T. (1968) The counting of lightning flashes, Tech. Rept. 49, SRI Project No. 4240, Contract No. DA 36-039-AMC-0040E, Stanford Research Institute; Menlo Park, Calif., 94 pp.

Appendix A

Remote Sensing Technique

The purpose of this appendix is to expand the information given in Section 2 on the sferics network. The network is comprised of signal monitors, which are electronic systems that detect and measure random occurring electromagnetic signals (sferics) produced by lightning discharges. Ten signal monitors were in operation during the period January to July 1972 and six during the remainder of the year. Six sensors are sufficient to monitor and record sferics on a global basis. As mentioned previously, this study was confined to the Eastern Hemisphere The signal monitor equipment and recording methodology, sferics-fix techniques, and the system threshold arrays will be explained. Although available, details of the electronic subsections of the signal monitors are considered beyond the scope of this study and will not be included.

A1. SIGNAL MONITOR EQUIPMENT

The signal monitor equipment is depicted in Figure A1. A vertical, non-directional whip antenna and two directional loop antennae are used to receive the sferic waveform. Although all electromagnetic signals appear on the antennae, the signal monitors record on a selective basis, using the criteria of waveform half-cycle characteristics, the relative threshold field intensity of the waveform, and the azimuth of arrival. The signal monitor also has the capability of recording

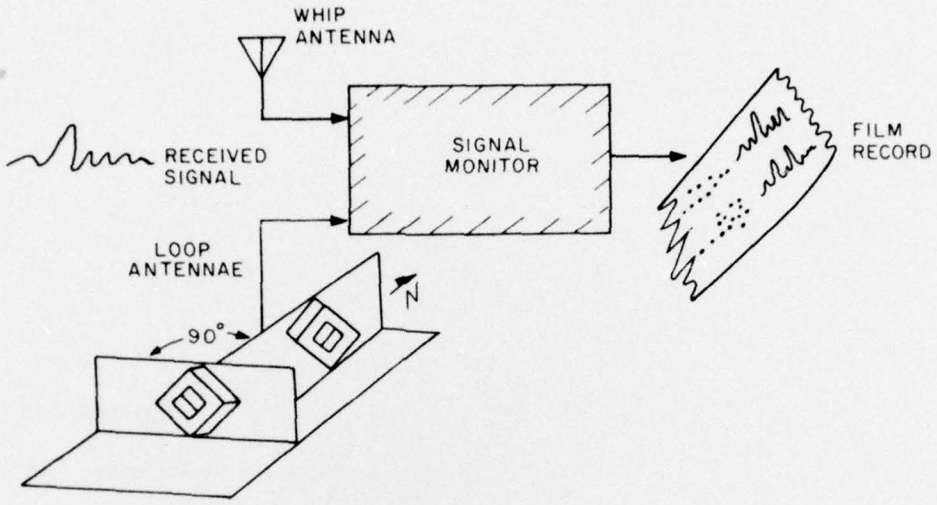

Figure A1. Signal Monitor Operation

signals selectively based on the energies of the distributed frequencies that compose the waveform. However, the spectrum analyzer section and the discriminant section which perform this function were not in operation during 1972. The individual waveforms, after analysis by the waveform and azimuth sections, were recorded to an accuracy of 10^{-5} seconds.

A typical recorded waveform is shown in Section 2 (Figure 1). The waveform has the appearance of a sine wave which builds to a peak and then decays to zero in 1000 μsec or less. The half-cycle of maximum amplitude of the recorded waveform occurs within the first 300 μsec of the waveform. The peak energies of all recorded sferics occur in the frequency range of 250 Hz to 60 kHz.

The whip antenna has a precise electrical length (2 m) for establishing the relative field intensity in volts per meter for each received waveform, irrespective of direction of propagation. Electromagnetic signals appearing across the antenna produce an output voltage proportional to its electrical height and the received signal intensity. The waveform input circuits receive the output of the vertical whip antenna. The signal monitor input, threshold control, peak detector and gate selector, and normalizing circuits in conjunction with the loop antennae and azimuth section circuits perform the prerecording criteria determinations previously described.

The loop antennae are used to resolve the received signal into two waveforms having an angular separation of 90 degrees. The two waveforms, in turn, produce coordinate voltages that are used to determine the received azimuth of the signal in degrees relative to true north. The azimuth accuracy approximates one degree with a full 360-degree coverage.

A2. SFERIC FIXING TECHNIQUE

The source location on earth of a sferic has been determined by the use of recording stations. The time of arrival of the sferic at each station was recorded to an accuracy of 10^{-5} sec. Then, the difference in time of arrival between stations was converted to distance by the use of the propagation rate at VLF. Although empirical tests were conducted to determine an optimum propagation rate, it was found that the speed of light was acceptable. The speed of light is the speed of propagation of electromagnetic radiation through a perfect vacuum. It is a universal, dimensional constant equal to $2.997925 \pm 0.000004 \times 10^{10}$ cm sec^{-1}.

Time fixes were obtained by a straightforward application of spherical trigonometry. Consider the case of three stations (I, J, and K) that receive a signal as shown below:

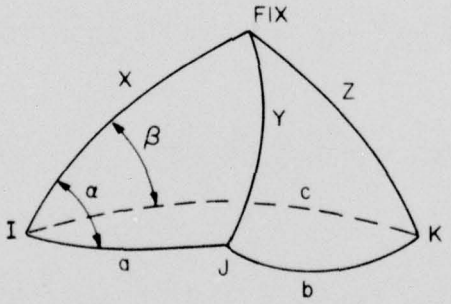

Station I receives the signal first. The distances between stations are represented by a, b, and c measured in radians and between the stations and the fix by X, Y, and Z as shown. We will develop formulas to find the angle α and the length of side X. This will locate the fix on the earth. From the differences of received times converted to distance using speed of light propagation, we can define:

1. $A = X - Y$
   $B = X - Z$

   thus

2. $Y = X - A$
   $Z = X - B$

   From the law of cosines we know that:

3. $\cos Y = \cos a \cos X + \sin a \sin X \cos \alpha$
   $\cos Z = \cos c \cos X + \sin c \sin X \cos \beta$

   Substituting in 3 the values of Y and Z from 2 gives:

4. $\cos (X - A) = \cos a \cos X + \sin a \sin X \cos \alpha$
   $\cos (X - B) = \cos c \cos X + \sin c \sin X \cos \beta$

   Expanding the left side of 4 gives us:

5. $\cos X \cos A + \sin X \sin A = \cos a \cos X + \sin a \sin X \cos \alpha$
   $\cos X \cos B + \sin X \sin B = \cos c \cos X + \sin c \sin X \cos \beta$

   Simplifying, we get:

6. $\cos X (\cos A - \cos a) + \sin X (\sin A - \sin a \cos \alpha) = 0$
   $\cos X (\cos B - \cos c) + \sin X (\sin B - \sin c \cos \beta) = 0$

   or:

7. $\tan X = \dfrac{\cos a - \cos A}{\sin A - \sin a \cos \alpha}$ and: $\tan X = \dfrac{\cos c - \cos B}{\sin B - \sin c \cos \beta}$

   clearly:

8. $\dfrac{\cos a - \cos A}{\sin A - \sin a \cos \alpha} = \dfrac{\cos c - \cos B}{\sin B - \sin c \cos \beta}$

   To simplify let

9. $P = \cos c - \cos B$
   and
   $R = \cos a - \cos A$

   Substituting 9 into 8 we get:

10. $R (\sin B - \sin c \cos \beta) = P (\sin A - \sin a \cos \alpha)$

    Also from the figure it can be seen that α and β differ by a constant which we will call CON which depends upon the configuration of stations used. Thus we may write:

11. $\beta = \alpha - CON$

Thus:

12. $R[\sin B - \sin c (\cos \alpha \cos (CON) + \sin \alpha \sin (CON))] = P \sin A - P \sin a \cos \alpha$

or:

13. $\sin \alpha (R \sin c \sin (CON)) + \cos \alpha (P \sin a - R \sin c \cos (CON) = (P \sin A - R \sin B)$

To further simplify let:

14. $S = R \sin c \sin (CON)$
$T = P \sin a - R \sin c \cos (CON)$ and
$Q = P \sin A - R \sin B$

Formula 13 then becomes

15. $S \sin \alpha + T \cos \alpha = Q$

Rewriting 15 in terms of cos α we have:

16. $S\sqrt{1 - \cos^2 \alpha} = Q - T \cos \alpha$

This is now squared to eliminate the radical:

17. $S^2(1 - \cos^2 \alpha) = Q^2 - 2QT \cos \alpha + T^2 \cos^2 \alpha$

Collecting terms:

18. $\cos^2 \alpha (T^2 + S^2) - 2QT \cos \alpha + (Q^2 - S^2) = 0$

This is a quadratic equation in cos α. It is solved using the quadratic formula to give the results:

19. $$\cos \alpha = \frac{2QT \pm \sqrt{4Q^2T^2 - 4(T^2 + S^2)(Q^2 - S^2)}}{2(T^2 + S^2)}$$

Using the values of cos α obtained in 19, we can find X, the distance from Station I to the fix by using formula 7.

The system of sensors consistently "fixed" the incoming sferics within the proper geographical area. In fact, frequent tests by Bailey[34] confirmed that the sferics were consistently fixed within 100 km of their true source location. As described in the discussion of the data, the datum points (counts of sferics) are valid for a large area bounded by a 10-degree latitude and 10-degree longitude block.

A3. THRESHOLD ARRAYS

The threshold arrays are system intensity values over a regularly spaced grid that represent the minimum field strength, expressed in decibels, below which no signal may be located and recorded. Figure A2 shows a portion of a threshold array.

55E	60E	65E	70E	75E	80E	85E	
56.4	55.2	54.1	53.7	53.9	54.7	53.6	40N
55.9	54.6	54.0	54.9	55.4	55.5	54.3	
55.5	54.4	55.3	56.2	56.9	55.8	54.7	30N
61.6	55.7	56.6	57.5	57.3	57.2	55.9	
63.0	61.7	57.9	58.6	58.6	58.1	56.8	20N
57.5	61.9	60.4	58.9	59.9	59.1	57 9	
59.0	60.0	61.1	62.1	61.5	60.2	60.0	10N
60.7	61.7	65.4	64.3	64.3	64.0	64.9	
62.4	67.7	66.5	65.8	65.6	66.6	66.2	EQ
70.1	68.8	67.6	66.4	67.1	68.0	68.9	
71.2	70.0	68.7	67.6	68.5	69.4	70.3	10S
72.3	71.1	69.9	69.1	68.9	70.8	71.8	
73.4	72.2	71.0	70.5	70.2	70.8	75.5	20S
74.5	73.3	72.2	72.0	71.5	73.7	77.0	
76.9	74.4	73.3	73.4	74.2	79.2	78.5	30S
78.0	75.5	76.0	75.0	81.4	80.7	80.0	
85.1	84.7	77.1	83.5	82.9	82.2	81.5	40S

Figure A2. Sample of a Threshold Array for Part of the Eastern Hemisphere. Values are in dB as defined in Section 3

The threshold arrays are the results of a model developed by the U.S. Air Force with the use of an IBM 360–65 computer. Figure A3 illustrates the process used to develop the arrays. There are two threshold arrays for 1972, covering the periods January to July and August to December. Two arrays are necessary due to a decrease in the number of sensors in the latter period. The model inputs are information about the sferics source (that is, field strength and location), information about the sensors (that is, location and average individual sensor thresholds, an attenuation table, and the number of sensors required to determine a fix). The model inputs and the model will be explained in greater detail.

A3.1 Model Inputs

The source information included sferic locations and field strengths. The source locations are regularly spaced grid points in five degree increments over the Eastern Hemisphere (see Figure A2). The initial sferic source field strengths are arbitrarily chosen values. The reason for this will become clear in the explanation of the model.

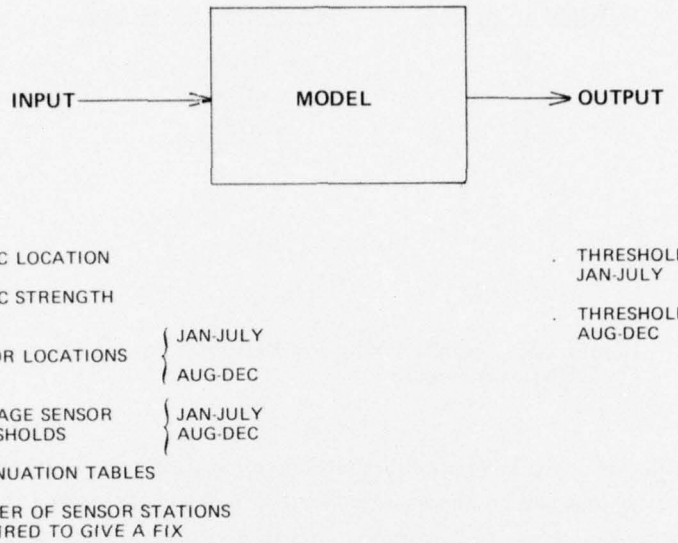

Figure A3. Illustration of the Process Used to Develop the Threshold Arrays

The sensor information is straightforward and requires little amplifying discussion. The individual sensor threshold values were determined by adding the operator-set threshold to the basic machine threshold, which is a constant 20 dB above a 1 mVm^{-1} field strength reference. The operator-set thresholds varied with thunderstorm activity. An incident sferic activity increased to a point that the sensor approached saturation, the operator increased his sensor threshold in 1-dB increments so that only the more intense sferics were recorded by his sensor. The resultant threshold values were recorded and averaged for each sensor over the two six-month periods (Jan to July and Aug to Dec) of 1972.

The signal loss from the source to the sensor due to attenuation was determined by using an empirically-derived table that was based on measurements conducted for the U.S. Air Force by the Denver Research Institute. The actual sensor equipment was used in the measurements. The main factor that affects propagation at VLF is the nature of the boundaries that form the wave guide; the earth's surface and the D-layer of the ionosphere. Table entries, as depicted in Figure A4, are averages of measurements that determined day vs night and land vs sea propagation results. The empirical table gives signal loss due to attenuation, expressed in decibels, for each one-thousand kilometer increment of propagation path. Table values are additive along the propagation path from the source to the sensor. Simple linear interpolation is used when necessary.

Distance (10^3 km)	Incremental Loss (dB)
1	1.5
2	1.8
3	2.3
4	2.1
5	2.4
6	2.0
.	.
.	.
.	.
.	.
.	.

Figure A4. Sample Table for Determining Signal Loss Due to Attenuation

The final model input is the number of sensor stations required to give a fix. At least three stations are required as a lower bound to determine a fix. Any number of stations may be used, however, up to the total number of stations in the system. A four-station fix was used during the 1972 period.

A3.2 The Model

The threshold arrays represent, on the average, the aggregate sensor or system sensitivity to sferics. As may be seen from Figure A2, each array entry represents the signal sensitivity value for a 5-degree, latitude-longitude block. The method by which a single value is obtained will be explained.

Consider for ease of explanation a hypothetical four sensor system, single source location, and threshold array values as shown in Figure A5. We assume further that a four-station fix is required to locate and record a sferic. We will discuss the method of obtaining the 61.4 dB value valid for the block centered at 54N 105E. We assume a spherical earth and choose an arbitrary signal field strength, in decibels, and a source location at the center of a given block. The path from the source to each sensor is then determined using spherical trigonometry. The signal loss, in decibels, is then calculated for each path using the attenuation table previously explained (Figure A4). The signal loss is subtracted from the source strength to give the strength of the signal upon arrival at each sensor site. This signal strength is compared with the sensor threshold value at each site. Since a "four-station fix" is required, the signal strength upon arrival at each of the four sensor locations must exceed the respective sensor thresholds to be recorded by the system. The source field strength is systematically increased in 0.1 dB increments until an associated, received signal strength is reached at each sensor site that exceeds each sensor threshold. The lowest such value for

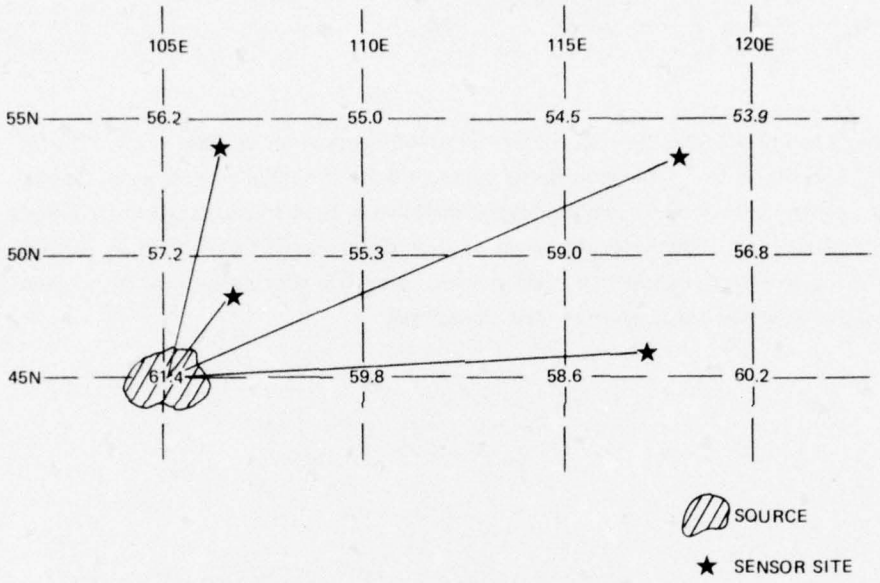

Figure A5. Illustration of the Method Used to Determine a Single Threshold-array Value (61.4 dB) using a Four Station Fix. Threshold values are in decibels as defined in Section 3

the 45N 105E grid point in Figure 4 is the 61.4 dB value, which represents the system threshold value. Other grid point values are determined in an identical manner. Figure A6 is a flow-chart depiction of model calculations.

The threshold arrays are used in the normalization of the sferics data. It is necessary to develop meaningful relative values for the counts of sferics over the grid since the sensitivity of the system of sensors to the collection of sferics is different for each grid point. The statistical distributions used in this study were assumed to follow the log-normal law. That is, the peak field strength of all received sferics follow a normal probability distribution about the mean (also the median) with values expressed in decibels, that is, on a logarithmic scale. The probability (Q) of occurrence of a sferic greater than or equal to a given threshold value (T_{ij}) at a grid point (i, j) may be expressed according to the log-normal law as

$$Q_{ij} = \frac{1}{\sigma\sqrt{2\pi}} \int_{T_{ij}}^{\infty} e^{-(T_{ij} - \bar{T})^2/2\sigma^2} \, dT$$

where σ is the standard deviation of received sferics in decibels and T is the threshold intensity. The grid point values of the threshold arrays are lower limits on the log-normal probability distribution used to normalize the counts of received sferics. Each sferic count at a grid point will be divided by the appropriate log-normal probability distribution value for that grid point to determine an estimate of the total sferics that occurred.

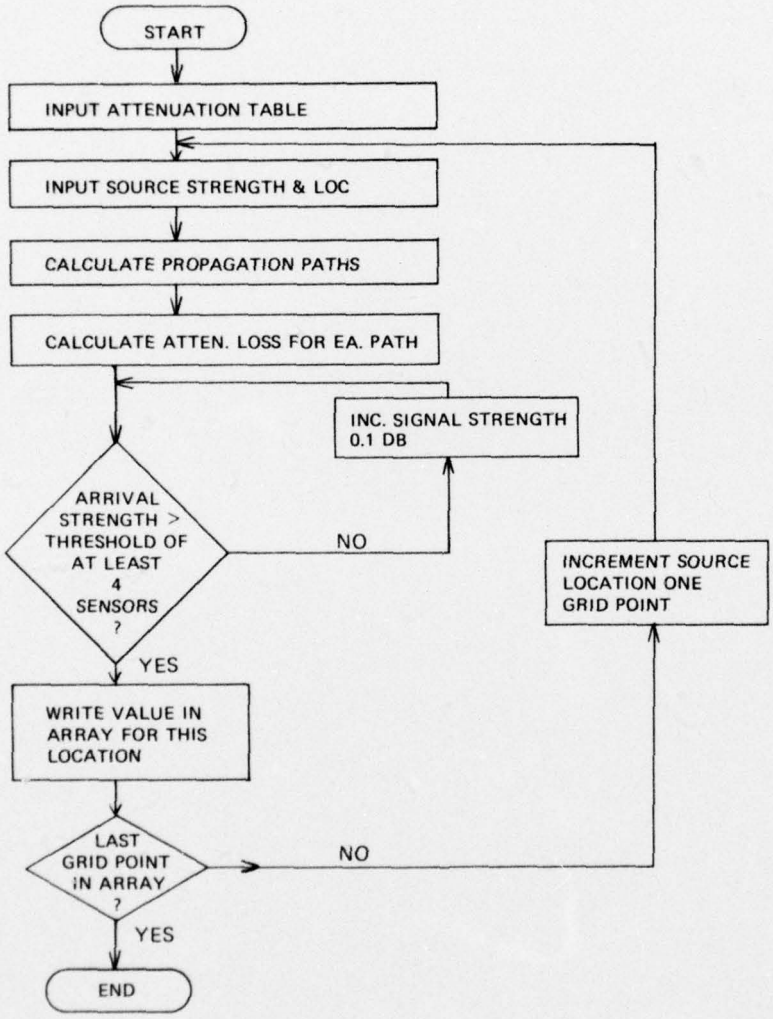

Figure A6. Flow Chart Depiction of Model Calculations Used to Determine the Threshold Arrays